Improved maps of surface water bodies, large dams, reservoirs, and lakes in China

Xinxin Wang[1, 2], Xiangming Xiao[2, *], Yuanwei Qin[2], Jinwei Dong[3], Jihua Wu[4], Bo Li[1, 5, *]

[1] Ministry of Education Key Laboratory for Biodiversity Science and Ecological Engineering, National Observations and Research Station for Wetland Ecosystems of the Yangtze Estuary, Institute of Biodiversity Science and Institute of Eco-Chongming, School of Life Sciences, Fudan University, Shanghai 200438, China. [2] Department of Microbiology and Plant Biology, Center for Earth Observation and Modeling, University of Oklahoma, Norman, OK 73019, USA. [3] Key Laboratory of Land Surface Pattern and Simulation, Institute of Geographic Sciences and Natural Resources Research, Chinese Academy of Sciences, Beijing 100101, China. [4] State Key Laboratory of Grassland Agro-Ecosystems, and College of Ecology, Lanzhou University, Lanzhou, Gansu 730000, China. [55]Yunnan Key Laboratory of Plant Reproductive Adaptation and Evolutionary Ecology and Centre for Invasion Biology, Institute of Biodiversity, School of Ecology and Environmental Science, Yunnan University, Kunming, Yunnan 650504, China.

Corresponding authors: Xiangming Xiao, xiangming.xiao@ou.edu; Bo Li, bool@fudan.edu.cn and bool@ynu.edu.cn

设置了格式：非上标/ 下标

设置了格式：下划线，字体颜色：超链接

带格式的：段落间距段后：0 磅

Abstract

Data and knowledge of surface water bodies (SWB), including large lakes and reservoirs (surface water areas > 1 km^2) are critical for the management and sustainability of water resources. However, the existing global or national dam datasets have large georeferenced coordinate offsets for many reservoirs, and some datasets have not reported reservoirs and lakes separately. In this study, we generated China's surface water bodies, Large Dams, Reservoirs, and Lakes (China-LDRL) dataset by analyzing all available Landsat imagery in 2019 (19,338 images) in Google Earth Engine and very-high spatial resolution imagery in Google Earth Pro. There were ~3.52 × 10^6 yearlong SWB polygons in China for 2019, only 0.01 × 10^6 of them (0.43%) were of large size (> 1 km^2). The areas of these large SWB polygons accounted for 83.54% of the total 214.92 × 10^3

28 km^2 yearlong surface water area (SWA) in China. We identified 2,~~140~~418 large dams, including
29 ~~1,494 reservoir~~624 off-stream dams and ~~646 river~~1,794 on-stream dams, ~~1,976~~2,194 large
30 reservoirs (16.~~42~~35 × 10^3 km^2), and 3,~~508~~051 large lakes (~~75.97~~73.38 × 10^3 km^2). In general, most
31 of the dams and reservoirs in China were distributed in South China, East China, and Northeast
32 China, whereas most of lakes were located in West China, the Lower Yangtze River Basin, and
33 Northeast China. The provision of the reliable, accurate China-LDRL dataset on ~~dams, large~~
34 reservoirs/dams and lakes will enhance our understanding of water resources management and
35 water security in China. The China-LDRL dataset is publicly available at
36 ~~https://doi.org/10.6084/m9.figshare.16964656.v2~~https://doi.org/10.6084/m9.figshare.16964656.v
37 3 (Wang et al., 2022).

~~1. Introduction~~

~~Surface water bodies (SWB), including large lakes and reservoirs (surface water areas > 1 km^2), play an important role in the control and management of water resources (Yang and Lu, 2014, 2013; Feng et al., 2013, 2019). A reservoir is usually defined as artificial lake formed by constructing dams across rivers (impoundment reservoir) (Thornton et al., 1996; Hayes et al., 2017) or partially or completely formed by enclosed waterproof banks with concrete or clay (off-stream reservoir) (Xiang et al., 2019; Thornton et al., 1996). Off-stream reservoirs usually include mountain and plain reservoirs (Fig. 1). Nearly 50% of the global large dams were built primarily for agricultural irrigation through storing, regulating, and diverting water~~ 1. Introduction

Surface water bodies (SWB), including large lakes and reservoirs (surface water areas > 1 km^2), play an important role in the control and management of water resources (Yang and Lu, 2014, 2013; Feng et al., 2013, 2019). A reservoir is usually defined as artificial lake formed by constructing dams across rivers (on-stream reservoir) (Thornton et al., 1996; Hayes et al., 2017) or partially or completely formed by enclosed waterproof banks with concrete or clay (off-stream reservoir) (Xiang et al., 2019; Thornton et al., 1996) (**Fig. S1**). Nearly 50% of the global large dams were built primarily for agricultural irrigation through storing, regulating, and diverting water (Mulligan et al., 2020)~~. Additionally, they are also used for hydropower generation, human and industrial uses, and flood peak attenuation (Lehner et al., 2011; Lehner and Döll, 2004; Wang et al., 2021a). Large lakes have been the subject of great interest not only because of their water~~

~~resources but also as indicators of local climate change and anthropogenic activities (Birkett and Mason, 1995; Ma et al., 2011), and they could provide vital ecosystem services for human being, such as alteration of river flow, supplies of irrigation water, fisheries, and abundant valuable mineral deposits, and have disproportionate effects on the global carbon cycle (Ran et al., 2021; Armstrong, 2010; Ma et al., 2011). Improved understanding of the detailed distributions of SWB, large dams, reservoirs, and lakes could provide crucial information on water resources, environmental health, status of ecosystems, and agricultural sustainability (Lehner and Döll, 2004).~~

. Additionally, they are also used for hydropower generation, human and industrial uses, and flood peak attenuation (Lehner et al., 2011; Lehner and Döll, 2004; Wang et al., 2021a). Large lakes have been the subject of great interest not only because of their water resources but also as indicators of local climate change and anthropogenic activities (Zhang et al., 2019; Ma et al., 2011; Birkett and Mason, 1995), and they could provide vital ecosystem services for human being, such as alteration of river flow, supplies of irrigation water, fisheries, and abundant valuable mineral deposits, and have disproportionate effects on the global carbon cycle (Ran et al., 2021; Armstrong, 2010; Ma et al., 2011). Improved datasets of the numbers, sizes, and spatial distributions of SWB, large dams, reservoirs, and lakes could substantially provide crucial inputs for the studies of water resources, environmental health, aquatic ecosystems, and agricultural sustainability (Lehner and Döll, 2004; Zhu et al., 2020).

Insert Fig. 1 here

~~China has the largest population, fastest-growing economy, increased expansion of irrigation,~~

~~relatively scarce water, dated infrastructure, and inadequate governance (Liu and Yang, 2012; Wang et al., 2020a; Tao et al., 2020). China encompasses almost 20% of the world's population but contains only 7% of the world's fresh water, and as the result, it has much smaller fresh water resource per capital than do most other countries (Feng et al., 2019; Dalin et al., 2014). Since 1980s, China has taken diverse measures to ensure the long-term water security~~ China has the largest population, fastest-growing economy, increased expansion of irrigation, limited water resource, dated water infrastructure, and inadequate water governance (Liu and Yang, 2012; Wang et al., 2020a; Tao et al., 2020). China encompasses almost 20% of the world's population but contains only 7% of the world's fresh water, and as the result, it has much smaller fresh water resource per capital than do most other countries (Feng et al., 2019; Dalin et al., 2014). Since 1980s, China has taken diverse measures to ensure the long-term water security (Zhou et al., 2020)~~. For example, China has a remarkable increase of reservoir construction across the country (Wang et al., 2021a), and the total dam number increased to ~89,700 by 2008 in China~~. For example, China has a remarkable increase of reservoir construction across the country (Wang et al., 2021a; Zhu et al., 2020), and the total number of dams increased to ~89,700 by 2008 in China (Yang and Lu, 2014)~~. The Three Gorges Reservoir, which is the world's largest hydroelectric dam (Three Gorges Dam), is fully operational for flood control, power generation, navigation, and water use (Wu et al., 2004; Zhang et al., 2012; Wang et al., 2013, 2020a). China also has a large number of lakes with tremendously cultural and economic importance. Previous study reported that there were 2,693 large lakes (area > 1 km^2) in China during 2005-2006, covering 0.9% of China's land area (Ma et al., 2011). However, due to intensive human activities and climate change over the last three~~

~~decades, several natural lakes have converted into reservoirs, accelerating dramatically shrinkage of lake areas (Yang and Lu, 2014; Ma et al., 2011). Therefore, the improved information on the distribution of large reservoirs and lakes in China is needed for assessing the impact of human activities and climate change on SWB, water management, and water security in China (Yang and Lu, 2014).~~

~~There are several~~. The Three Gorges Reservoir, which is the world's largest hydroelectric dam (Three Gorges Dam), is fully operational for flood control, power generation, navigation, and water use (Wu et al., 2004; Zhang et al., 2012; Wang et al., 2013, 2020a). China also has a large number of lakes with tremendously cultural and economic importance (Ma et al., 2011; Zhang et al., 2019). A previous study reported that there were 2,693 large lakes (area > 1 km^2) in China during 2005-2006, covering 0.9% of China's land area (Ma et al., 2011). However, due to intensive human activities and climate change over the last three decades, several natural lakes have converted into reservoirs, dramatically accelerating shrinkage of lake areas (Yang and Lu, 2014; Ma et al., 2011). Therefore, the improved datasets on the number, size, and spatial distribution of large reservoirs and lakes in China is needed for assessing the impact of human activities and climate change on SWB, water management, and water security in China (Zhu et al., 2020; Yang and Lu, 2014).

Several published global dam and reservoir datasets ~~that~~ include information from China (**Table 1**). The World Register of Dams (WRD), which was ~~published~~organized and released by the International Commission on Large Dams (ICOLD, 2011), is the largest and widely-used

dataset ~~(Mulligan et al., 2020; Paredes-Beltran et al., 2021; Wang et al., 2021a).~~(Mulligan et al., 2020; Paredes-Beltran et al., 2021; Wang et al., 2021a). It reports 23,841 dam entries for China, however, a large proportion of those entries are not georeferenced with latitude and longitude information, which limits its wide ~~application (Wang et al., 2021a).~~applications (Wang et al., 2021a). The GlObal ~~geOreferenced~~GeOreferenced Database of Dams (GOODD) V1 dataset reported 9,234 georeferenced dams in China (Mulligan et al., 2020), however, the information (e.g. area, volume capacity) of ~~all~~ the corresponding reservoirs was not reported. The FAO's (Food and Agriculture Organization of the United Nations) global information system on water resources and agricultural water management (AQUASTAT) lists 14,000 dams in the world, ~~but~~in which only part of 722 dams in China were georeferenced, and has not been updated since 2015. The Global Reservoir and Dam database (GRanD), developed by the Global Water System Project (GWSP), compiled the available reservoir and dam information globally (Lehner et al., 2011) and has been updated for the year 2019. However, it only lists 922 geolocated dam entries for China. Recently, ~~Wang et al. (2021a)~~Wang et al. (2021a) released a global Georeferenced global dam and reservoir (GeoDAR) dataset with 5,~~347~~283 georeferenced dams in China, and the reservoirs had more than 40 attributes acquired from the WRD dataset. ~~However, our preliminary quality check of the dataset shows that the georeference information of many dams in the GeoDAR dataset has moderate to substantial shifts (or offsets, mis-location), up to 500m or more (**Fig. S1**), indicating further improvement is needed before it can be used for geospatial analysis. There were also some~~In April 2022, the newest and fully peer-reviewed version of GeoDAR is available, and this newest version had high accuracy of dams in China (**Fig. S2**). There were also several published

dam and reservoir maps at the national scale (**Table. 1**), but these maps neither included georeferenced dams nor reported reservoir attributes (e.g. reservoir area).

Table 1. Information on published dam and reservoir datasets for the globe and China.

Name	Spatial domain	Number of dams in the globe	Number of dams in China	Georeferenced dam?	Reservoir information (area …)?
WRD	Global	~ 60000	23,841	Either not georeferenced or inaccessible.	Yes, > 40 attributes
GOODD V1	Global	38667	9,231	Yes	No
FAO AQUASTAT	Global	14000	722	Partly georeferenced	Yes, reservoir capacity and area
GRanD	Global	7320	922	Yes	Yes, ~ 50 attributes
GeoDAR	Global	23680	5,~~345~~283	Yes	Yes, attributes from WRD dataset
CLRM	China	/	89,700	No	Yes, reservoir capacity and area
BFNCW	China	/	98,002	No	No

WRD: the World Register of Dams (https://www.icold- cigb.org); GOODD: GlObal geOreferenced Database of Dams (Mulligan et al., 2020); FAO AQUASTAT: The Food and Agriculture Organization of the United Nations (FAO) global information system on water resources and agricultural water management (http://www.fao.org/aquastat/en/databases/dams/); GRanD: the Global Reservoir and Dam database (Lehner et al., 2011); GeoDAR: Georeferenced global dam and reservoir dataset ~~(Wang et al., 2021a)~~(Wang et al., 2021a); CLRM: China's Lakes and Reservoirs Map (Yang and Lu, 2014); BFNCW: Bulletin of First National Census for Water from Ministry of Water Resources the People's Republic of China (http://www.mwr.gov.cn/2013pcgb/index.html). "/" means these data were published in China, but global dam information is unavailable.

In addition to the dam and reservoir datasets, several studies have reported the spatial distribution and multi-year dynamics of inland SWB ~~(Tao et al., 2020; Ma et al., 2011; Wang et al., 2020a; Feng et al., 2019) and lakes (Gao, 2015; Gao et al., 2012; Yang and Lu, 2014; Ma et al., 2011) in China, however, they did not explicitly explore the spatial distribution of large reservoirs and lakes in China, making it impossible to assess the impact of human activities on these two types of water resources (Yang and Lu, 2014).~~(Tao et al., 2020; Ma et al., 2011; Wang et al., 2020a; Feng et al., 2019) and lakes (Gao, 2015; Gao et al., 2012; Ma et al., 2011; Zhang et al., 2019) in China, however, they did not explicitly explore the spatial distribution of large reservoirs and lakes in China, making it impossible to assess the impact of human activities on these two types of water resources. Thus, to date, the spatial distributions of SWB, large dams, reservoirs, and lakes in China have not been fully investigated and documented, yet.

~~The objective of this study was to produce detailed and accurate maps of open SWB, large dams, reservoirs, and lakes (surface water area > 1 km^2) in China in 2019, the latest year when this study started in late 2020. First, this study used time-series Landsat imagery in 2019 and Google Earth Engine (GEE) cloud computing platform as well as the simple and robust surface water mapping algorithm (Zou et al., 2018, 2017; Zhou et al., 2019b; Wang et al., 2020a) to generate raster maps of SWB in China at 30-m spatial resolution. Second, we converted the raster map of SWB to a vector map of SWB and identified those large SWB with area > 1 km^2. Third, we combined the vector map of SWB with the historical satellite images in 2019 within China in~~

~~Google Earth Pro to identify dams and released China's surface water bodies, large dams, reservoirs, and lakes dataset, namely, China-LDRL. Forth, we analyzed the spatial distribution of SWB, large dams, reservoirs, and lakes in China. Finally, we discussed the reliabilities, uncertainties, limitations, outlooks, and implications of the China-LDRL dataset.~~

~~2. Materials and Methods~~

~~2.1 Study area~~

~~The study area covered all the provincial-level administrative divisions in China (**Fig. 2a**~~The objective of this study was to produce detailed and accurate maps of open SWB, large dams, reservoirs, and lakes (surface water area > 1 km^2) in China in 2019, the latest year when this study started in late 2020, and those SWB with area ≤ 1km^2 were excluded. First, this study used time-series Landsat imagery in 2019 and Google Earth Engine (GEE) cloud computing platform as well as the simple and robust surface water mapping algorithm (Zou et al., 2018, 2017; Zhou et al., 2019b; Wang et al., 2020a) to generate raster maps of SWB in China at 30-m spatial resolution. Second, we converted the raster map of SWB to a vector map of SWB and identified those large SWB with area > 1 km^2. Third, we combined the vector maps of SWB with the historical satellite images in 2019 within China in Google Earth Pro to identify dams and released China's surface water bodies, large dams, reservoirs, and lakes dataset, namely, China-LDRL. Forth, we analyzed the spatial distribution of SWB, large dams, reservoirs, and lakes in China. Finally, we discussed

the reliabilities, uncertainties, limitations, outlooks, and implications of the China-LDRL dataset for the study of water security.

2. Materials and Methods

2.1 Study area

The study area covered all the provincial-level administrative divisions in China (**Fig. 1a**), including 23 provinces, 2 special administrative regions (Hong Kong and Macao), 4 municipalities (Beijing, Tianjin, Shanghai, and Chongqing), and 5 Autonomous Regions (Inner Mongolia, Guangxi, Tibet, Ningxia, and Xinjiang). Since Macao and Hong Kong have relatively small areas and are very close to Guangdong Province, we combined them as one region (Guangdong) when we performed the statistical analysis in this study.

China has great altitude diversity as the eastern plains and southern coasts consist of lowlands and foothills, the southern areas of China consist of hilly and mountainous terrains, the west and north of the country are dominated by basins, plateaus, and massifs, and the southwestern China contains part of the highest tablelands on earth, the Tibetan Plateau (**Fig. 1a**). Due to substantial differences in latitude, longitude, and altitude, the climate of China is extremely diverse, ranging from tropical in the far south to subarctic in the far north and alpine in the higher elevations of the Tibetan Plateau, contributing to the much more surface water areas in Southwest and Southeast of China than other regions, especially North China (Wang et al., 2020a).

Insert Fig. 1 here

2.2 Data

2.2.1 Landsat data

In this study, we used the available Landsat surface reflectance (SR) images in the GEE platform, and there was a total of 19,338 images in 2019 for China, including 9,028 Landsat-7 ETM+ images and 10,310 Landsat-8 OLI images (~21.73 TB). The detailed information of Landsat SR products is available on the GEE platform (https://developers.google.com/earth-engine/datasets/catalog/landsat, last access: 18 February 2022). All these images had undergone necessary pre-processing in GEE, including radiometric calibration ~~and~~, atmospheric correction, and the removal of stripes in Landsat-7 imagery. We used the quality assurance (QA) band that was generated by the CFMASK algorithm (Zhu et al., 2015) to identify bad-quality observations, including clouds and cloud shadows (Murray et al., 2019; Pekel et al., 2016). We also used the Shuttle Radar Topography Mission (SRTM) digital elevation model (DEM) data, the solar azimuth and zenith angle data of each image, and ee.Terrain.hillShadow algorithm in GEE to identify those pixels with terrain shadows ~~(Zou et al., 2018; Wang et al., 2020a) (**Fig. 2b**~~(Zou et al., 2018; Wang et al., 2020a) (**Fig. 1b**), which were excluded from the data analysis. Out of ~132.43 million pixels in China, approximately 98.36% had more than 5 good-quality observations and 91.24% had more than 10 good-quality observations in 2019. About 93.14% of the 78.9 million pixels in North China

had more than 20 good-quality observations due to the overlapping of Landsat images at the high latitudes and less cloud cover ~~(Zhou et al., 2019a; Wang et al., 2020b)~~(Zhou et al., 2019a; Wang et al., 2020b). Note that the number of Landsat-7 ETM+ images in GEE may change in the future, as USGS continues to work with the International Ground stations (IGS) in the world to assemble and rescue some images from individual stations. For Landsat-8 OLI images, USGS does not rely on IGS for image downlink, as its data record is able to store all the images and then downlink them to the Landsat archive (Wulder et al., 2016).

We used three spectral indices (NDVI, EVI, mNDWI) to identify SWB in this study. These indices are defined as:

$$NDVI = \frac{\rho_{nir}-\rho_{red}}{\rho_{nir}+\rho_{red}} \quad (1)$$

$$EVI = 2.5 \times \frac{\rho_{nir}-\rho_{red}}{\rho_{nir}+6\times\rho_{red}-7.5\times\rho_{blue}+1} \quad (2)$$

$$mNDWI = \frac{\rho_{green}-\rho_{swir}}{\rho_{green}+\rho_{swir}} \quad (3)$$

where ρ_{blue}, ρ_{green}, ρ_{red}, ρ_{nir}, and ρ_{swir} are blue, green, red, near-infrared, and shortwave infrared bands of Landsat images, respectively.

~~**Insert Fig. 2 here**~~

2.2.2 Dam and reservoir datasets

The GlObal GeOreferenced Database of Dams (GOODD) dataset was released in 2020 and it lists ~38,000 georeferenced dams as well as derived data on their associated catchments through one by one degree titles on the Google Earth geobrowser during 2007-2011 and the Shuttle Radar

Topography Mission (SRTM) Water Body Dataset (SWBD) (Mulligan et al., 2020). It provides the raw digitized coordinates for the locations of dam walls, but it does not provide the detailed attribute data on the characteristics of each dam and reservoir (**Fig. ~~3a~~2a, d**). Both the large dams and medium sized dams were captured in this dataset.

The Global Reservoir and Dam (GRanD) Database v1.3 was recently updated in February 2019 by Lehner et al. (2011) (**Fig. ~~3b~~2b, e**). The spatial information of these dams was contributed by eleven participating institutions. Each dam was assigned to a polygon that depicted the reservoir surface, which was provided by SWBD (v1.1) and the surface water maps were produced by the Joint Research Center (JRC) of the European Commission from Landsat imagery at 30-m spatial resolution for the period 1984-2015 (Pekel et al., 2016) (v1.3). All reservoirs with a storage capacity of more than 0.1 km^3 were included in this dataset, and some smaller reservoirs were also added when their data were available.

The Georeferenced global Dam And Reservoir dataset (GeoDAR) was produced by utilizing multi-source dam and reservoir inventories (ICOLD WRD and GRanD v1.3 datasets) and the Google Maps geocoding API ~~(Wang et al., 2021a) (Fig. 3d~~(Wang et al., 2021a) (**Fig. 2d, e**). The GeoDAR product includes two successive versions. GeoDAR v1.0 is essentially a georeferenced subset of ICOLD WRD, and contains more than 20,000 dam entries, and each of which is indexed by an encrypted identifier (ID) that is associated with a WRD record, allowing for the potential retrieval of all its 40+ proprietary attributes from ICOLD. GeoDAR v1.1 consists of (1) dam entries as in v1.0 except those that further harmonized with GRanD for an improved inclusion of the

largest dams, and (2) reservoir boundaries for most of the dam entries. The GeoDAR was just updated in April 2022 and is available at https://doi.org/10.5281/zenodo.6163413.

Insert Fig. ~~3~~2 here

2.3 Methods

The workflow for producing the China-LDRL dataset included two major ~~two~~ sections: 1) generation of yearlong SWB maps in China by analyzing time-series Landsat imagery in 2019 with GEE platform, and 2) identification of dams and classification of yearlong SWB into lakes, reservoirs, and rivers by analyzing the historical satellite images in 2019 within China in Google Earth Pro. A flowchart showing the methodology of this study is illustrated in **Fig. ~~4~~3**.

Insert Fig. ~~4~~3 here

2.3.1 Algorithm to generate annual ~~map~~maps of yearlong surface water bodies

In this study, we combined a surface water index (mNDWI) and two greenness-based vegetation indices (EVI and NDVI) to identify SWB through the algorithm of ((mNDWI > EVI or mNDWI > NDVI) and EVI < 0.1) (Eq. (4)). This mNDWI/VIs algorithm can reduce the effects of vegetation on identification of SWB, and ~~was widely~~has already been used to identify and map SWB at the regional and national scales with high accuracy ~~(Zou et al., 2018, 2017; Zhou et al., 2019b; Wang et al., 2020a)~~(Zou et al., 2018, 2017; Zhou et al., 2019b; Wang et al., 2020a). Furthermore, this mNDWI/VIs algorithm had been compared with other surface water body mapping algorithms (e.g. NDWI, mNDWI, TCW, and AWEI), and the results showed that ~~this~~the

integration of mNDWI/VIs algorithm and Landsat images could identify SWB with high producer's accuracy (98.1%) and user's accuracy (91.0%) (Zhou et al., 2017).

Surface water body frequency (F_{SWB}) of a pixel in a year was calculated as the ratio of the number of observations identified as surface water body to the number of good-quality observations in a year and ~~scaled~~ranged from 0 to 1.0 (or 100%) (Zou et al., 2017), see Eq. (5). We generated the F_{SWB} map of all the pixels in China for 2019 in the GEE platform (**Fig. 5a**).

$$SWB = \begin{cases} 1, & \text{(mNDWI>EVI or mNDWI>NDVI) and EVI<0.1} \\ 0, & \text{Other values} \end{cases} \quad (4)$$

$$F_{SWB} = \frac{N_{SWB}}{N_{good}} \quad (5)$$

where SWB is surface water body, F_{SWB} is surface water body frequency, N_{SWB} is the number of observations identified as SWB (see Eq. (4)) in 2019, N_{good} is the number of good-quality observations in 2019.

~~Consistent with our previous publications (Zou et al., 2018; Wang et al., 2020a), a water pixel was defined as yearlong surface water ($F_{SWB} \geq 0.75$), seasonal surface water ($0.05 \leq F_{SWB} < 0.75$), or ephemeral surface water ($F_{SWB} < 0.05$). We generated the seasonal and yearlong SWB maps in China for 2019, respectively (**Fig. 5b, c**).~~

~~**Insert Fig. 5**~~Consistent with our previous studies (Zou et al., 2018; Wang et al., 2020a), a water pixel was defined as yearlong surface water body ($F_{SWB} \geq 0.75$), seasonal surface water body ($0.05 \leq F_{SWB} < 0.75$), or ephemeral surface water body ($F_{SWB} < 0.05$). We generated the seasonal and yearlong SWB maps in China for 2019, respectively (**Fig. 4b, c**).

Insert Fig. 4 here

2.3.2 The procedure to identify dams, reservoirs, and lakes in Google Earth Pro

We first generated the yearlong SWB vector map in China for 2019 based on the yearlong SWB raster map, then reprojected it to the Krasovsky_1940_Albers equal-area conic projection and calculated the area (km^2) of each yearlong SWB polygon ~~within China~~as its attribute (Python code is available in: https://drive.google.com/drive/folders/1B19VKbCIoDPmu-IcmiZcOIUF8wi1YnE?usp=sharing). When we reported large reservoirs and lakes, only ~~polygon~~those polygons with area > 1 km^2 ~~was~~were kept in this study~~.~~ **(Fig. S3).** In an effort to distinguish riverine or off-~~channel~~stream reservoirs from lakes, we uploaded the large SWB vector ~~layer~~layers into Google Earth Pro, and checked whether a dam existed around each polygon through the historical satellite images in 2019 within China by visual image interpretation approach. If a dam did not exist, we classified the polygon as river or lake; if a dam ~~did~~does exist, we classified the polygon ~~would be classified~~ as on-stream reservoir (constructed on a river/stream regardless of impoundment ~~reservoir~~) or off-stream reservoir~~.~~ (formed by partial or complete embankment around an off-stream lake) **(Fig. S1).** Simultaneously, ~~we classified~~ the corresponding ~~dams~~dam would be classified as ~~river dams~~on-stream dam or ~~reservoir dams~~off-stream dam. Finally, the SWB polygons were classified into lakes, reservoirs, and rivers, and the dams/reservoirs were classified into ~~reservoir dams~~on-stream and ~~river~~off-stream dams/reservoirs (**Fig. ~~4~~3**). This work was carried out and completed by the lead author (Dr. Wang) over ~~one month~~two months, and users could reproduce the dam dataset by uploading the SWB polygons in

the historical satellite images in 2019 in Google Earth Pro and following the procedure described here. Note that satellite images in the Google Earth Pro may change over time, but such change may have very limited impact on identification of ~~dam~~dams as ~~dam~~dams have often ~~exists over~~stayed for many years after ~~its~~their construction.~~–~~

~~**2.4 Calculation of lake and reservoir attributes**~~

~~The areas (km^2) of SWB polygons were generated using the Krasovsky_1940_Albers coordinate system. As we generated the vector maps of yearlong and seasonal SWB in China for 2019, we calculated the yearlong SWB areas linked to the dams as the reservoir areas. Likewise, we also calculated each lake area as its attribute in our study.~~

~~2.5~~2.4 Cross-comparison with other lake and reservoir datasets

To better understand the improvements and potential ~~application~~applications of our China-LDRL dataset, we compared it with other three available dam and reservoir datasets: the GOODD, GRanD V1.3, and GeoDAR datasets (**Fig. ~~3~~2**). We first compared the dam quantity and areas of large ~~reservoir~~reservoirs at the provincial and national scales. Then, we checked the spatial distribution of each dam from these datasets within Google Earth imagery as all these datasets provide detailed georeferenced coordinates for some of dams, and the georeferenced information could be directly acquirable from the spatial longitude and latitude. Here we did not compare the reservoir area with the GOODD dataset as it does not provide such attribute except for catchment area (**Fig. ~~3d~~2d**).

3. Results

3.1 Annual map of surface water bodies in China for 2019

Surface water body frequency (F_{SWB}) of individual pixels for 2019 varied substantially across China (**Fig. ~~5~~4**). There were ~3.38 million seasonal surface water pixels (30-m spatial resolution) in China, amounting to ~3,375.88 × 10^3 km^2 seasonal surface water area (SWA) in 2019. Xinjiang Province had the largest seasonal SWA (751.14 × 10^3 km^2), followed by Tibet (600.70 × 10^3 km^2), Qinghai (564.57 × 10^3 km^2), Inner Mongolia (511.42 × 10^3 km^2), and Heilongjiang Province (343.33 × 10^3 km^2) (**Fig. ~~6a~~5a**). There were ~0.21 million yearlong surface water pixels in China for 2019, amounting to ~214.92 × 10^3 km^2 yearlong SWA, which were mainly located in Tibet (62.65 × 10^3 km^2), Qinghai (41.08 × 10^3 km^2), and Xinjiang (24.60 × 10^3 km^2) Provinces (**Fig. ~~6b~~5b**). Additionally, Heilongjiang, Jiangsu, Inner Mongolia, Hubei, and Anhui Provinces also had ~~relative~~relatively larger yearlong SWA (> 5 × 10^3 km^2) than other provinces in China.

Insert Fig. ~~6~~5 here

3.2 Numbers and areas of yearlong surface water bodies with different sizes in China

The numbers and areas of yearlong SWB polygons of different sizes in China differed considerably for 2019 (**Fig. ~~7~~6**). In terms of yearlong SWB numbers, out of a total of 3.52 × 10^6 yearlong SWB polygons in China in 2019, approximate 3.51 × 10^6 polygons (99.57%) had an area of ≤ 1 km^2, and ~2.16 × 10^6 polygons (61.19%) had an area of ≤ 0.0036 km^2 (covering only 2 × 2 Landsat grid cells). Only 15 × 10^3 (0.43%) yearlong SWB polygons had an area of > 1 km^2, and

359 polygons had an area of > 100 km^2. In terms of yearlong SWB areas, out of a total of 214.92 × 10^3 km^2 yearlong SWA in China in 2019, large SWB polygons (size > 1 km^2) accounted for 83.54%, and very large SWB polygons (size > 100 km^2) accounted for 52.48%.

The numbers and areas of yearlong SWB polygons of different sizes at the provincial scale had similar distribution patterns with those at the national scale (**Fig. ~~S2, S3~~S4, S5**). Almost all the yearlong SWB polygons in individual provinces had an area of ≤ 1 km^2 (**Fig. ~~S2~~S4**), however, those SWB polygons with an area of > 1 km^2 accounted for a large proportion of SWA in most provinces (**Fig. ~~S3~~S5**). Those yearlong SWB polygons with an area of > 100 km^2 were mostly very large lakes and rivers, ~~and they~~which were mainly located in Tibet, Xinjiang, Qinghai, Jiangxi, and Heilongjiang Provinces (**Fig. ~~S3~~S5**) (Feng et al., 2019). Some provinces also had very large-size reservoirs, such as Miyun Reservoir in Beijing, whose polygon size was greater than 100 km^2.

Insert Fig. ~~7~~6 here

3.3 Numbers, areas, and distribution of large dams, reservoirs, and lakes in China

We identified 2,~~140~~418 large dams in China, including ~~1,494 reservoir~~624 off-stream dams and ~~646 river~~1,794 on-stream dams, most of which were located in South, East, and Northeast China, as well as ~~Tianshan Mountains in~~ Xinjiang of Northwest China (**Fig. ~~8a~~7a**). At the provincial scale, ~~Heilongjiang Province~~Xinjiang had the largest number of ~~reservoir~~off-stream dams (~~148~~67), followed by Shandong (~~147), Hubei (143), Guangdong (122~~62), Heilongjiang (46), and ~~Jilin (121~~Anhui (45) Provinces. ~~There were also five~~Three provinces (~~Xinjiang~~Hubei, Yunnan,

~~Liaoning, Henan,~~ and ~~Anhui)~~ Guangdong) also had relatively larger ~~reservoir~~off-stream dam numbers ~~(> 50~~(≥ 40) than other provinces. ~~Shanghai (1), Tibet (1), and~~ Chongqing, Qinghai ~~Province (2)~~, and Tibet had ~~very small numbers of reservoir~~no off-stream dams ~~(< 5)~~ (**Fig. ~~8b~~7b**). Most of ~~river~~on-stream dams in China were distributed in those provinces with large rivers. Guangdong had the largest number of ~~river~~on-stream dams (~~90~~172) in China, followed by Hubei (146), Heilongjiang (132), Shandong (112), Jilin (103), and Sichuan (~~84), Hunan (58), Fujian (43), and Yunnan Province (40).~~103) Provinces (**Fig. 7c**). However, there were no ~~river~~on-stream dams in ~~Jiangsu and~~ Shanghai ~~(**Fig. 8c**).~~. In terms of the functions of two kinds of dams and the spatial patterns of climate (e.g. precipitation, temperature) and social-economic factors (e.g. population, GDP, irrigation area) in South and North China, the provinces in Northeast and East China had larger percentage of ~~reservoir~~off-stream dams, whereas the provinces in Northeast and South ~~and Southwest~~ China had larger percentage of ~~river~~on-stream dams (**Fig. ~~8d~~7d**).

Insert Fig. ~~8~~7 here

China had 3,~~508~~051 large lakes with an area of > 1 km^2 in 2019, most of which were distributed in West China, the Lower Yangtze River Basin, and Northeast China (**Fig. ~~9a, S4~~8a, S6**), and they together amounted to ~~75.97~~73.38 × 10^3 km^2. Tibet in West China had the largest ~~lake~~ number ~~(978~~of lakes (966), followed by Qinghai (~~482~~479), Xinjiang (~~388~~350), Inner Mongolia (~~241~~234), and ~~Hubei Province (218)~~Heilongjiang (174) Provinces (**Fig. ~~9b~~8b**). The lake areas in China had similar spatial patterns with the lake numbers (**Fig. ~~9c~~8c**), and the western provinces in China had much larger lake areas than other provinces, especially Tibet and Qinghai

Provinces with ~~32.51~~31.73 × 10^3 km^2 and ~~16.47~~15.78 × 10^3 km^2, respectively. As reservoirs and dams usually exist simultaneously, the spatial patterns of reservoir numbers and areas matched well with those of dam numbers (**Figs. ~~8b, 9c~~7b, 8c-f**). In total, China had ~~1,976~~2,194 large reservoirs in 2019, they together amounted to an area of ~16.~~42~~35 × 10^3 km^2. ~~Hubei Province~~Xinjiang in ~~Northeast~~Northwest China had the largest reservoir area (~~2177.96~~1,923.11 km^2), followed by ~~Jilin (1,323.29 km^2),~~ Heilongjiang (1,~~320.40~~468.48 km^2), Jiangsu (1,309.95 km^2), and ~~Henan Province (1304.60~~Hubei (1,190.75 km^2~~).~~) Provinces. In contrast, Tibet (18.34 km^2), Shanghai (36.~~14~~61 km^2), and ~~Taiwan Province (54.89~~Ningxia (45.40 km^2) had much smaller reservoir areas than other provinces in China. In general, most of the dams and reservoirs in China were distributed in South China, East China, and Northeast China, whereas most of lakes were located in West China, the Lower Yangtze River Basin, and Northeast China ~~(Figs. 8, 9).~~.

Insert Fig. ~~9~~8 here

4. Discussion

4.1 Improvements of the dataset of large dams, reservoirs, and lakes in China

In order to validate the reliability of our China-LDRL dataset, we first compared the numbers of large dams and areas of large reservoirs between our dataset and published datasets (GOODD, GRanD, and GeoDAR), then we checked the geographical coordinates of dams within the historical satellite images in 2019 in Google Earth Pro.

The GOODD dataset has the largest number of dams (9,~~231~~234) in China among these

published global datasets (**Fig. ~~10a~~2a**). However, it includes both large, moderate, and small dams, and does not report the corresponding reservoir attributes (e.g. reservoir area), which limits its applications to water-related research (Paredes-Beltran et al., 2021). The GRanD dataset has the smallest number (814) of large dams with reservoir area > 1 km^2 in China (**Fig. ~~10b~~9b, e**) as the dam information was provided by multiple institutions from the world (Lehner et al., 2011), which clearly underestimates the number of dams. The GeoDAR dataset has a larger number of large dams (~~993~~1,162) than the GRanD dataset, because it was generated by combining the GRanD and ICOLD WRD datasets ~~(Wang et al., 2021a).~~(Wang et al., 2021a). However, our China-LDRL dataset identified 2,~~140~~418 large dams and ~~1,976~~2,194 large reservoirs (**Fig. ~~10d~~9d, e~~, f~~**), making substantial improvement of large dam and reservoir dataset in China.

The number differences of large dams between our China-LDRL and the GRanD and GeoDAR datasets could be explained by several factors. First, our study used all the available Landsat images in 2019 and a more accurate SWB mapping algorithm to generate SWB maps in China, however, the GRanD and GeoDAR datasets used the SWBD map (produced in 2000) (Slater et al., 2006) and the surface water maps during 1984-2015 produced by the JRC (Pekel et al., 2016)~~, thus, we could~~. We were able, therefore, to integrate more Landsat images and get more SWB polygons, as well as larger numbers of large dams and reservoirs than other datasets. In addition, the different strategies for identifying dams also caused the differences of dam numbers. The dam information from the GRanD dataset was contributed by eleven participating institutions, and the GeoDAR dataset combined two published dam datasets (WRD and GRanD~~) and~~),

rechecked detailed dam information~~,~~ using the Google Maps geocoding API, and then reported the georeferenced information of dams. Unlike the GRanD and GeoDAR datasets, our study first generated SWB raster and vector maps using the mNDWI/VIs SWB mapping algorithm, and then selected the large yearlong SWB polygons with area > 1 km^2. After that, we visually checked the large SWB polygons one by one and identified each dam with accurate geographical coordinates (**Fig. S3**). In addition to the dam numbers, we also compared the reservoir areas between different datasets (**Fig. ~~S~~S7**). Our China-LDRL dataset reported ~16.35 × 10^3 km^2 large reservoir area, which was smaller than those of the GRanD (20.98 × 10^3 km^2) and GeoDAR (21.84 × 10^3 km^2) datasets. The GRanD v1.3 dataset linked the "maximum surface water extent" from the JRC dataset to the corresponding dams as the reservoir regions, however, we used the "yearlong surface water body" to depict the reservoirs in the China-LDRL dataset, which might have made our reservoir areas smaller (**Fig. S8**).

Insert Fig. ~~10 here~~

~~9In addition to the dam numbers, we also compared the reservoir areas between different datasets (Fig. 11). Our China-LDRL dataset reports ~16.42 × 10^3 km^2 large reservoir area, which was smaller than those of the GRanD (20.98 × 10^3 km^2) and GeoDAR (21.84 × 10^3 km^2) datasets. We checked the reservoir polygons of the three datasets in Google Earth Pro, and found that some large lakes were identified as reservoirs by the GranD and GeoDAR datasets, such as the Hongze Lake in Jiangsu Province (Fig. S5a), contributing to the overestimate of reservoir areas. In addition, the GRanD v1.3 dataset linked the "maximum surface water extent" from the JRC dataset to the~~

~~corresponding dams as the reservoir regions, however, we used the "yearlong surface water body" to depict the reservoir in the China-LDRL dataset, which caused our smaller reservoir areas (**Fig. S5b-c**).~~

~~**Insert Fig. 11** **here**~~

In this study, we also checked the accuracy of geographical coordinates of dams from these dam datasets. Here we first uploaded above-mentioned three dam datasets and our China-LDRL dataset in the Google Earth Pro and visually checked the spatial distribution of each dam within the historical satellite images in 2019 (**Fig. ~~12~~10**). We found that the dam locations of the GOODD dataset had substantial geographic offsets, some of which are larger than 500 m (**Fig. ~~S6~~S9**). We further overlapped the GOODD dam layer with our yearlong SWB map (Section 2.3.1), and the results showed that only 12.52 ± 3.87% of the GOODD dams were intersected with the SWB layer at the national scale (**Fig. ~~13a~~S10a**). In the case that we applied a 100-m and 500-m tolerance when intersecting the GOODD dams with our yearlong SWB map for 2019, the intersection rate increased to only 47.58 ± 9.70% and 76.46 ± 7.11%, respectively (**Figs. ~~13b, S7~~S10b, S11**). In addition, we applied different tolerances when ~~intersecting~~ the GRanD and GeoDAR datasets intersected with our yearlong SWB layer. About 65.57 ± 6.79% of the dams in the GRanD dataset ~~were~~ intersected with our yearlong SWB map ~~(**Fig. 13a**).~~, which increased to 87.52 ± 6.45% and 95.94 ± 4.49% when using a 100-m and 500-m tolerance ~~(**Figs. 13b, S7**).~~. Although the GeoDAR dataset is ~~released by integrating~~ just updated and the ~~GRanD dataset~~newest version had much higher accuracy than the previous version, its geographical coordinates also had ~~larger~~some offsets

(**Fig. ~~12d, f~~10f, g**), and ~~41.10~~58.49 ± 6.~~13~~07% of its dams ~~were~~ intersected with the yearlong SWB layer, and ~~63.18 ± 5.61% and 86.69~~82.33 ± 3.~~74~~98% and 90.22 ± 3.18% intersected when the tolerance was 100-m and 500-m ~~**(Figs. 13b, S7)**. These comparisons suggested~~. Different methods and purposes caused the ~~substantial geographic~~georeferenced offsets of these ~~published~~ datasets ~~(~~. For example, the original digitized dam points in GOODD~~, GRanD, and~~ V1.0 were purposefully snapped to the 30-arc-second HydroSHEDS river networks, leading to the offset from the actual dam locations. On the other hand, GOODD v1.0 is directly compatible with HydroSHEDS and is therefore more convenient for modeling purposes. In GeoDAR~~), and~~ v1.1, dam points in China were georeferenced using the Google Maps geocoding API, and many dam labels fell on the reservoir surface instead of the dams. Additionally, Google Maps in China have substantial misalignment (500 m to 1 km or so) between the satellite images and the map labels due to China's GPS shift problem, resulting in the geographic offsets even though the geocoding procedure is correct. In total, these comparisons suggested the improved accuracy of our China-LDRL dataset, which could provide important and reliable information for water resource management and water security in China.

Insert Fig. ~~12 here~~

~~Insert Fig. 13~~10 here

设置了格式: 字体: 加粗

4.2 Uncertainties, limitations, outlooks, and implications

In this study, we produced detailed and more accurate China's open surface water bodies, large

dams, reservoirs, and lakes (China-LDRL) dataset for 2019, and analyzed their spatial distribution patterns. This study benefited from the usage of time-series Landsat imagery and GEE cloud computing platform, as well as simple and robust SWB mapping algorithms. First, time series Landsat images at high spatial resolution (30-m) provide larger numbers of good-quality observations for identifying SWB. Second, GEE cloud computing platform enables us to acquire and analyze tens of thousands of Landsat images in hours. Third, the mNDWI/VIs algorithm used in this study ~~could reduce~~reduced the uncertainties induced by the bad-quality observations and provide accurate SWB maps. Finally, we visually checked the large SWB polygons (area > 1 km^2) one by one by using the historical satellite images in 2019 within China in Google Earth Pro, and we recorded the georeferenced coordinates of individual dams in China for 2019.

We would also acknowledge that the data quality of input satellite images remains to be a concern for the identification of dams, reservoirs, and lakes. The spatial distribution of good-quality observations of Landsat data shows that more than 98.36% of the total 30-m pixels in China had more than 5 good-quality observations and more than 91.24% of the total pixels had more than 10 good-quality observations for 2019 (**Fig. ~~2b~~1b**), but the regions with complex topography and mountains, such as South and Southwest China, had much fewer good-quality observations than other regions, which might underestimate surface water areas, as well as dam and reservoir numbers and areas. In addition, it is impossible to remove all the bad-quality observations (e.g. clouds, terrain shadows) because of the limited quality of the QA band and digital elevation model data in GEE. Therefore, the remaining bad-quality observations could result in some inevitable

uncertainties in the resultant maps. In the future, as more images from Landsat dataset and other high spatial resolution sensors (e.g., Sentinel-1, Sentinel-2) are added into GEE platform (Wulder et al., 2016), SWB mapping accuracy could be further improved, providing more detailed geospatial data of dams, reservoirs, and lakes in China. In addition, visual interpretation method for identifying dams and reservoirs in this study could also bring about some uncertainties to the classification of dams/reservoirs due to the limitations of knowledge and experience of interpreters, such as the misclassification of some reservoirs regulated by dams/gates as lakes (e.g. Hongze Lake in Jiangsu Province) and the misclassification between on-stream and off-stream dams/reservoirs.

In our China-LDRL dataset, we identified and reported those large SWB, however, the importance of monitoring small water bodies (area $\leq$ 1 km^2) and dams is gradually recognized as they play critical roles in accurate assessments of their agricultural potential or their cumulative influence ~~in~~on watershed hydrology (Ogilvie et al., 2018). In the ~~near~~ future, we can include these small SWB polygons into our dataset to enhance the spatial details and distributions of dams, reservoirs, and lakes in China.

The conversions between rivers, lakes, and reservoirs have critical effects on the ecosystem services. For example, the construction of the Three Gorges Dam contributed to the decrease of surface water area and biodiversity in its downstream areas (Fang et al., 2006; Feng et al., 2013; Wang et al., 2020a), and reduced the sediment loads in the Yangtze River, causing the decreased deposition rates of coastal wetlands in the Yangtze Delta ~~(Feng et al., 2016; Wang et al.,~~

2021b)(Feng et al., 2016; Wang et al., 2021b). Furthermore, the conversion from natural lakes and rivers to man-made reservoirs has disproportionate effects on the local, regional, and global carbon cycle (Howard Coker et al., 2009). For example, dam construction has reduced the areal extent of CO_2 gas exchange in natural rivers (Ran et al., 2021). In the future, more detailed information (e.g. construction year of dam) couldneeds to be included in our China-LDRL dataset, making it possible to analyze the effects of conversions from natural lakes and rivers to reservoirs on the biodiversity and carbon cycle.

5. Data availability

The China-LDRL dataset is publicly available at https://doi.org/10.6084/m9.figshare.16964656.v2https://doi.org/10.6084/m9.figshare.16964656.v3 (Wang et al., 2022), and it includes three shapefiles. The "China_large_dams_attribute.shp" is the large dams in China, as well as their with five attributes (, including ID, (dam_id), dam class, (dam_class, "1" means on-stream dam and "-1" means off-stream dam), longitude and, latitude, polygon area, and corresponding reservoir ID (reser_id). The "China_large_lakes.shp" is the large lakes map in China with three attributes: ID, lake area (poly_area, km^2), and lake perimeter (poly_len, km). The "China_large_reservoirs.shp" areis the large lakes andreservoirs map in China with five attributes: ID, reservoir maps in China.area (poly_area, km^2), reservoir perimeter (poly_len, km), corresponding dam ID (dam_ID), and dam classes (dam_class).

6. Code availability

Code used in calculations of surface water bodies is available upon request. ~~Code for transferring the images to vector maps in Python could be found in: https://drive.google.com/drive/folders/1B19VKbCIoDPmu-IcmiZcOIUF8wi1YnE?usp=sharing.~~

7. Conclusion

Several studies have published global or national dam, reservoir, and lake datasets based on satellite images (**Table 1**). However, these datasets usually have large georeferenced coordinate offsets, which poses some limitations to those studies that aim to address major issues in hydrology, ecology, and water resource management in China. In this study, we have generated the dataset of China's open surface water bodies, large dams, reservoirs, and lakes (China-LDRL) for 2019, and then analyzed their spatial distributions at the provincial and national scales. Satellite image data quality is still a major source of uncertainty that affects the accuracy of the surface water body maps. As more images from Landsat datasets and other high spatial resolution sensors (e.g., Sentinel-1, Sentinel-2) are added ~~into~~to GEE platform, the accuracy of SWB maps can be further improved, providing more detailed geospatial data of dams, reservoir, and lakes in China. The provision of the reliable, accurate China-LDRL dataset on dams, reservoirs, and lakes will contribute to the understanding of water ~~crisis and water~~ resources management and water security in China.

Author ~~contribution~~contributions

X.X., X.W., and B.L. designed the study. X.W. carried out image data processing and led interpretation of the results and writing of the manuscript. Y.Q., and J.D. contributed to image data processing, X.X., B.L., Y.Q., J.D., and J. W. contributed to the interpretation and discussion of the results.

Declaration of Competing Interest

The authors declare that they have no known competing financial interests or personal relationships that could have appeared to influence the work reported in this paper.

Acknowledgements

This study was supported in part by research grants from the U.S. National Science Foundation (1911955), the Natural Science Foundation of China (81961128002), the China Postdoctoral Science Foundation (2021M700835 and 2021TQ0072), and the China Scholarship Council (201906100124).

References

Armstrong, A.: Lake carbon, Nat. Geosci., 3, 151, https://doi.org/10.1038/ngeo816, 2010.

Birkett, C. M. and Mason, I. M.: A New Global Lakes Database for a Remote Sensing Program Studying Climatically Sensitive Large Lakes, J. Great Lakes Res., 21,

https://doi.org/10.1016/S0380-1330(95)71041-3, 1995.

Dalin, C., Hanasaki, N., Qiu, H., Mauzerall, D. L., and Rodriguez-Iturbe, I.: Water resources transfers through Chinese interprovincial and foreign food trade, Proc. Natl. Acad. Sci. U. S. A., 111, 9774–9779, https://doi.org/10.1073/pnas.1404749111, 2014.

Fang, J., Wang, Z., Zhao, S., Li, Y., Tang, Z., Yu, D., Ni, L., Liu, H., Xie, P., Da, L., Li, Z., and Zheng, C.: Biodiversity changes in the lakes of the Central Yangtze, https://doi.org/10.1890/1540-9295(2006)004[0369:BCITLO]2.0.CO;2, 2006.

Feng, L., Hu, C., Chen, X., and Zhao, X.: Dramatic inundation changes of China's two largest freshwater lakes linked to the Three Gorges Dam, Environ. Sci. Technol., 47, 9628–9634, https://doi.org/10.1021/es4009618, 2013.

Feng, L., Han, X., Hu, C., and Chen, X.: Four decades of wetland changes of the largest freshwater lake in China: Possible linkage to the Three Gorges Dam?, Remote Sens. Environ., 176, 43–55, https://doi.org/10.1016/j.rse.2016.01.011, 2016.

Feng, S., Liu, S., Huang, Z., Jing, L., Zhao, M., Peng, X., Yan, W., Wu, Y., Lv, Y., Smith, A. R., McDonald, M. A., Patil, S. D., Sarkissian, A. J., Shi, Z., Xia, J., and Ogbodo, U. S.: Inland water bodies in China: Features discovered in the long-term satellite data, Proc. Natl. Acad. Sci. U. S. A., 116, 25491–25496, https://doi.org/10.1073/pnas.1910872116, 2019.

Gao, H.: Satellite remote sensing of large lakes and reservoirs: from elevation and area to storage, Wiley Interdiscip. Rev. Water, 2, 147–157, https://doi.org/10.1002/wat2.1065, 2015.

Gao, H., Birkett, C., and Lettenmaier, D. P.: Global monitoring of large reservoir storage from satellite remote sensing, Water Resour. Res., 48, W09504, https://doi.org/10.1029/2012WR012063, 2012.

Hayes, N. M., Deemer, B. R., Corman, J. R., Razavi, N. R., and Strock, K. E.: Key differences between lakes and reservoirs modify climate signals: A case for a new conceptual model, Limnol. Oceanogr. Lett., 2, 47–62, https://doi.org/https://doi.org/10.1002/lol2.10036, 2017.

Howard Coker, E., Hotchkiss, R. H., and Johnson, D. A.: Conversion of a Missouri River Dam and Reservoir to a Sustainable System: Sediment Management1, JAWRA J. Am. Water Resour. Assoc., 45, 815–827, https://doi.org/https://doi.org/10.1111/j.1752-1688.2009.00324.x, 2009.

ICOLD: World register of dams, Paris, 2011.

Lehner, B. and Döll, P.: Development and validation of a global database of lakes, reservoirs and wetlands, J. Hydrol., 296, 1–22, https://doi.org/10.1016/j.jhydrol.2004.03.028, 2004.

Lehner, B., Liermann, C. R., Revenga, C., Vörömsmarty, C., Fekete, B., Crouzet, P., Döll, P., Endejan, M., Frenken, K., Magome, J., Nilsson, C., Robertson, J. C., Rödel, R., Sindorf, N., and Wisser, D.: High-resolution mapping of the world's reservoirs and dams for sustainable river-flow management, Front. Ecol. Environ., 9, 494–502, https://doi.org/10.1890/100125, 2011.

Liu, J. and Yang, W.: Water sustainability for China and beyond, Science (80-.)., 337, 649–650, https://doi.org/10.1126/science.1219471, 2012.

Ma, R. H., Yang, G. S., Duan, H. T., Jiang, J. H., Wang, S. M., Feng, X. Z., Li, A. N., Kong, F. X., Xue, B., Wu, J. L., and Li, S. J.: China's lakes at present: Number, area and spatial distribution, Sci. China Earth Sci., 54, 283–289, https://doi.org/10.1007/s11430-010-4052-6, 2011.

Mulligan, M., van Soesbergen, A., and Sáenz, L.: GOODD, a global dataset of more than 38,000 georeferenced dams, Sci. Data, 7, 1–8, https://doi.org/10.1038/s41597-020-0362-5, 2020.

Murray, N. J., Phinn, S. R., DeWitt, M., Ferrari, R., Johnston, R., Lyons, M. B., Clinton, N., Thau, D., and Fuller, R. A.: The global distribution and trajectory of tidal flats, Nature, 565, 222, https://doi.org/10.1038/s41586-018-0805-8, 2019.

Ogilvie, A., Belaud, G., Massuel, S., Mulligan, M., Le Goulven, P., and Calvez, R.: Surface water monitoring in small water bodies: Potential and limits of multi-sensor Landsat time series, Hydrol. Earth Syst. Sci., 22, 4349–4380, https://doi.org/10.5194/hess-22-4349-2018, 2018.

Paredes-Beltran, B., Sordo-Ward, A., and Garrote, L.: Dataset of Georeferenced Dams in South America (DDSA), Earth Syst. Sci. Data, https://doi.org/10.5194/essd-13-213-2021, 2021.

Pekel, J. F., Cottam, A., Gorelick, N., and Belward, A. S.: High-resolution mapping of global surface water and its long-term changes, Nature, 540, 418, https://doi.org/10.1038/nature20584, 2016.

Ran, L., Butman, D. E., Battin, T. J., Yang, X., Tian, M., Duvert, C., Hartmann, J., Geeraert, N., and Liu, S.: Substantial decrease in CO2 emissions from Chinese inland waters due to global

change, Nat. Commun., 12, 1–9, https://doi.org/10.1038/s41467-021-21926-6, 2021.

Slater, J. A., Garvey, G., Johnston, C., Haase, J., Heady, B., Kroenung, G., and Little, J. K.: The SRTM Data Finishing Process and Products, Photogramm. Eng. Remote Sensing, 72, 237–247, 2006.

Tao, S., Zhang, H., Feng, Y., and Zhu, J.: Changes in China's water resources in the early 21st century, Front. Ecol. Environ., https://doi.org/10.1002/fee.2164, 2020.

Thornton, J., Steel, A., and Rast, W.: Chapter 8* - Reservoirs, in: Water quality assessments : a guide to the use of biota, sediments and water in environmental monitoring, 2–3, 1996.

Wang, J., Sheng, Y., Gleason, C. J., and Wada, Y.: Downstream Yangtze River levels impacted by Three Gorges Dam, Environ. Res. Lett., 8, 044012, https://doi.org/10.1088/1748-9326/8/4/044012, 2013.

Wang, J., Walter, B. A., Yao, F., Song, C., Ding, M., Maroof, A. S., Zhu, J., Fan, C., Xin, A., McAlister, J. M., Sikder, S., Sheng, Y., Allen, G. H., Crétaux, J.-F., and Wada, Y.: GeoDAR: Georeferenced global dam and reservoir dataset for bridging attributes and geolocations, Earth Syst. Sci. Data, 2021, 1–52, https://doi.org/10.5194/essd-2021-58, 2021a.

Wang, X., Xiao, X., Zou, Z., Dong, J., Qin, Y., Doughty, R. B., Menarguez, M. A., Chen, B., Wang, J., Ye, H., Ma, J., Zhong, Q., Zhao, B., and Li, B.: Gainers and losers of surface and terrestrial water resources in China during 1989 – 2016, Nat. Commun., 11, 1–12, https://doi.org/10.1038/s41467-020-17103-w, 2020a.

672 Wang, X., Xiao, X., Zou, Z., Hou, L., Qin, Y., Dong, J., Doughty, R. B., Chen, B., Zhang, X.,
673 Chen, Y., Ma, J., Zhao, B., and Li, B.: Mapping coastal wetlands of China using time series
674 Landsat images in 2018 and Google Earth Engine, ISPRS J. Photogramm. Remote Sens., 163,
675 312–326, https://doi.org/10.1016/j.isprsjprs.2020.03.014, 2020b.

676 Wang, X., Xiao, X., Xu, X., Zou, Z., Chen, B., Qin, Y., Zhang, X., Dong, J., Liu, D., Pan, L., and
677 Li, B.: Rebound in China's coastal wetlands following conservation and restoration, Nat.
678 Sustain., 4, 1076–1083, https://doi.org/10.1038/s41893-021-00793-5, 2021b.

679 Wu, J., Huang, J., Han, X., Gao, X., He, F., Jiang, M., Jiang, Z., Primack, R. B., and Shen, Z.:
680 The Three Gorges Dam: An ecological perspective, Front. Ecol. Environ., 2, 241–248,
681 https://doi.org/10.1890/1540-9295(2004)002[0241:TTGDAE]2.0.CO;2, 2004.

682 Wulder, M. A., White, J. C., Loveland, T. R., Woodcock, C. E., Belward, A. S., Cohen, W. B.,
683 Fosnight, E. A., Shaw, J., Masek, J. G., and Roy, D. P.: The global Landsat archive: Status,
684 consolidation, and direction, Remote Sens. Environ., 185, 271–283,
685 https://doi.org/10.1016/j.rse.2015.11.032, 2016.

686 Xiang, Y., Fu, Z., Meng, Y., Zhang, K., and Cheng, Z.: Analysis of wave clipping effects of
687 plain reservoir artificial islands based on MIKE21 SW model, Water Sci. Eng., 12, 179–187,
688 https://doi.org/https://doi.org/10.1016/j.wse.2019.08.002, 2019.

689 Yang, X. and Lu, X.: Drastic change in China's lakes and reservoirs over the past decades, Sci.
690 Rep., 4, 6041, https://doi.org/10.1038/srep06041, 2014.

691 Yang, X. and Lu, X. X.: Delineation of lakes and reservoirs in large river basins: An example of
692 the Yangtze River Basin, China, https://doi.org/10.1016/j.geomorph.2013.02.018, 2013.

693 Zhang, G., Yao, T., Chen, W., Zheng, G., Shum, C. K., Yang, K., Piao, S., Sheng, Y., Yi, S., Li,
694 J., Oreilly, C., Qi, S., Shen, S., Zhang, H., and Jia, Y.: Regional differences of lake evolution
695 across China during 1960s-2015 and its natural and anthropogenic causes, Remote Sens.
696 Environ., 221, 386–404, https://doi.org/10.1016/j.rse.2018.11.038, 2019.

697 Zhang, Q., Li, L., Wang, Y. G., Werner, A. D., Xin, P., Jiang, T., and Barry, D. A.: Has the
698 Three-Gorges Dam made the Poyang Lake wetlands wetter and drier?, Geophys. Res. Lett., 39,
699 L20402, https://doi.org/10.1029/2012GL053431, 2012.

700 Zhou, F., Bo, Y., Ciais, P., Dumas, P., Tang, Q., Wang, X., Liu, J., Zheng, C., Polcher, J., Yin,
701 Z., Guimberteau, M., Peng, S., Ottle, C., Zhao, X., Zhao, J., Tan, Q., Chen, L., Shen, H., Yang,
702 H., Piao, S., Wang, H., and Wada, Y.: Deceleration of China's human water use and its key
703 drivers, Proc. Natl. Acad. Sci. U. S. A., 117, 7702–7711,
704 https://doi.org/10.1073/pnas.1909902117, 2020.

705 Zhou, Y., Dong, J., Xiao, X., Xiao, T., Yang, Z., Zhao, G., Zou, Z., and Qin, Y.: Open surface
706 water mapping algorithms: A comparison of water-related spectral indices and sensors, 9, 256,
707 https://doi.org/10.3390/w9040256, 2017.

708 Zhou, Y., Dong, J., Liu, J., Metternicht, G., Shen, W., You, N., Zhao, G., and Xiao, X.: Are there
709 sufficient Landsat observations for retrospective and continuous monitoring of land cover

changes in China?, Remote Sens., 11, https://doi.org/10.3390/rs11151808, 2019a.

Zhou, Y., Dong, J., Xiao, X., Liu, R., Zou, Z., Zhao, G., and Ge, Q.: Continuous monitoring of lake dynamics on the Mongolian Plateau using all available Landsat imagery and Google Earth Engine, Sci. Total Environ., 689, 366–380, https://doi.org/10.1016/J.SCITOTENV.2019.06.341, 2019b.

Zhu, J., Song, C., Wang, J., and Ke, L.: China's inland water dynamics: The significance of water body types, Proc. Natl. Acad. Sci., 117, 13876–13878, https://doi.org/10.1073/pnas.2005584117, 2020.

Zhu, Z., Wang, S., and Woodcock, C. E.: Improvement and expansion of the Fmask algorithm: Cloud, cloud shadow, and snow detection for Landsats 4-7, 8, and Sentinel 2 images, Remote Sens. Environ., 159, 269–277, https://doi.org/10.1016/j.rse.2014.12.014, 2015.

Zou, Z. H., Dong, J. W., Menarguez, M. A., Xiao, X. M., Qin, Y. W., Doughty, R. B., Hooker, K. V, and Hambright, K. D.: Continued decrease of open surface water body area in Oklahoma during 1984-2015, Sci. Total Environ., 595, 451–460, https://doi.org/10.1016/j.scitotenv.2017.03.259, 2017.

Zou, Z. H., Xiao, X. M., Dong, J. W., Qin, Y. W., Doughty, R. B., Menarguez, M. A., Zhang, G. L., and Wang, J.: Divergent trends of open-surface water body area in the contiguous United States from 1984 to 2016, Proc. Natl. Acad. Sci. U. S. A., 115, 3810–3815, https://doi.org/10.1073/pnas.1719275115, 2018.

729

730

731

732

733 **Figures and** ~~figure legends~~**Legends**

设置了格式：字体：Times New Roman，小四，加粗

带格式的：正文，段落间距段后：10 磅，行距：2 倍行距

734

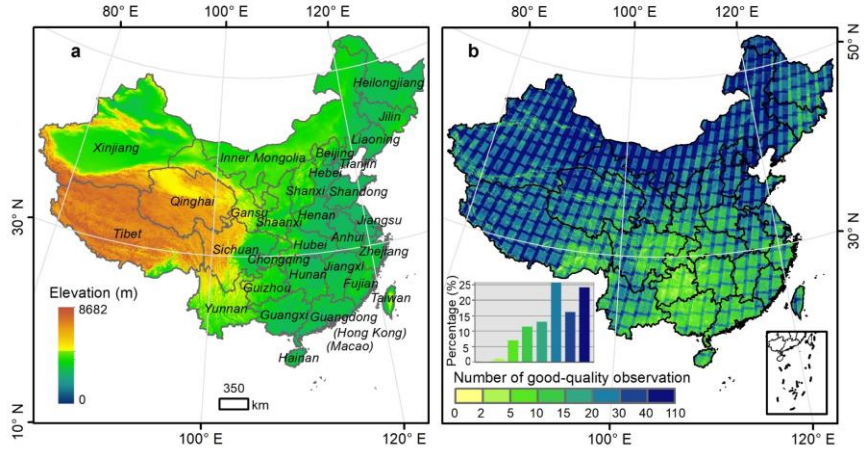

735

736 **Fig. 1.** ~~Types of reservoirs in China within high-resolution images (© Google Earth Pro 2019). (a~~

737 ~~b) Impoundment reservoir; (c-d) Mountain reservoir; (e-f) Plain reservoir.~~

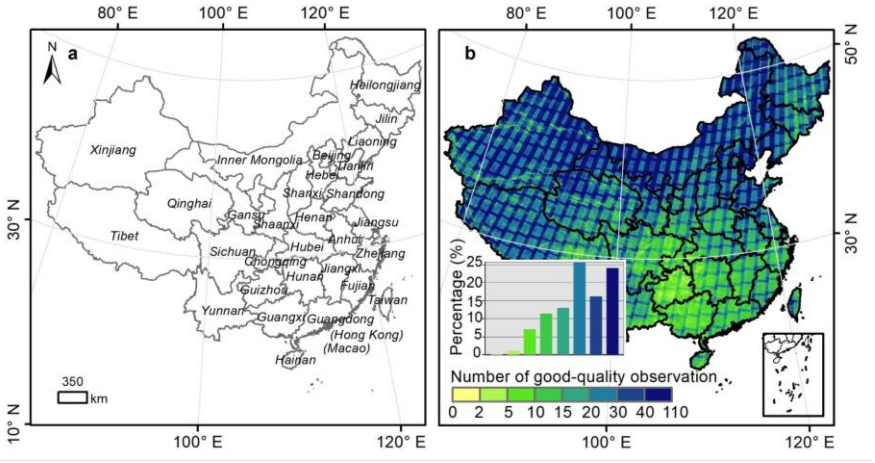

738

739 ~~Fig. 2.~~ Spatial distribution of provinces and elevation (a) and numbers of Landsat good-quality

740 observations (b) in China for 2019.

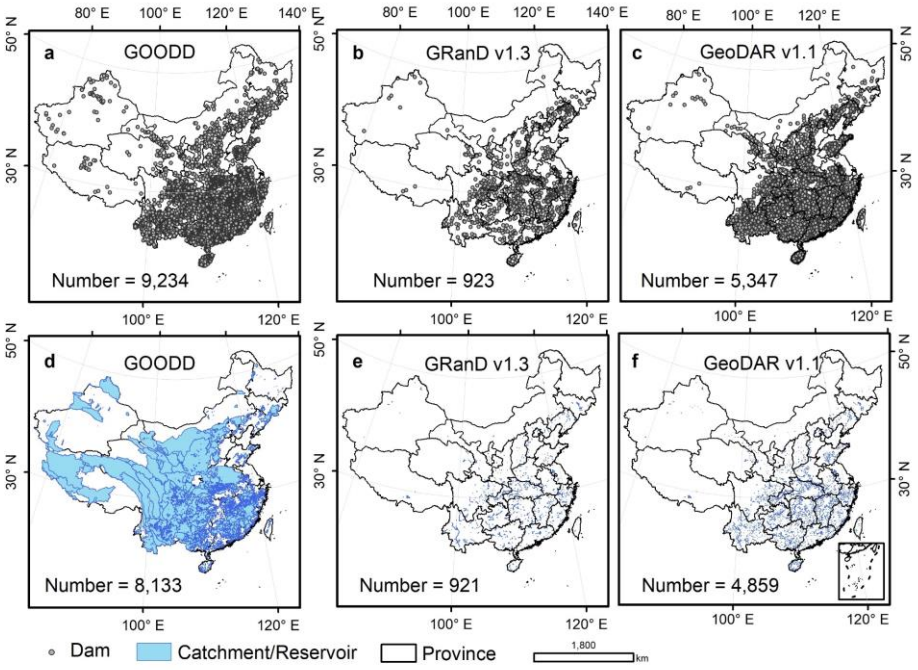
a
GOODD
Number = 9,234
b
GRanD v1.3
Number = 923
c
GeoDAR v1.1
Number = 5,347
d
GOODD
Number = 8,133
e
GRanD v1.3
Number = 921
f
GeoDAR v1.1
Number = 4,859
80° E
100° E
120° E
140° E
50° N
30° N
Dam
Catchment/Reservoir
Province
1,800
km

741

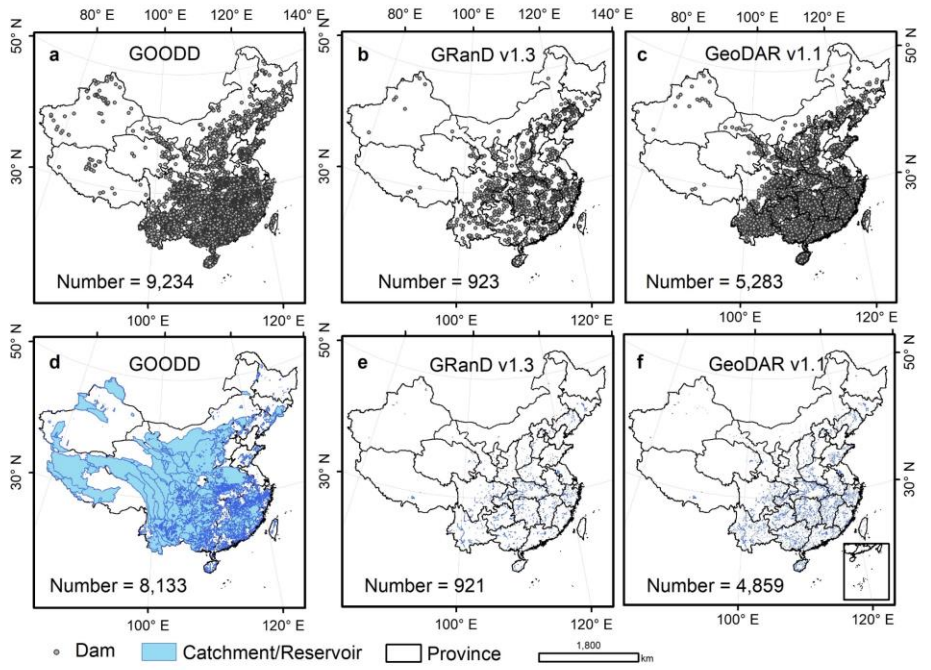

Fig. ~~3~~2. Spatial distribution of dams from the GlObal GeOreferenced Database of Dams (GOODD) (a~~) (Mulligan et al., 2020~~), the Global Reservoir and Dam (GRanD) v1.3 (b~~) (Lehner et al., 2011~~), and the Georeferenced global Dam And Reservoir (GeoDAR) v1.1 (c) ~~(Wang et al., 2021)~~ datasets. The GOODD dataset reported the catchment of each dam (d) while the GRanD and GeoDAR datasets reported the reservoir information of each dam (e, f).

设置了格式：字体：非加粗

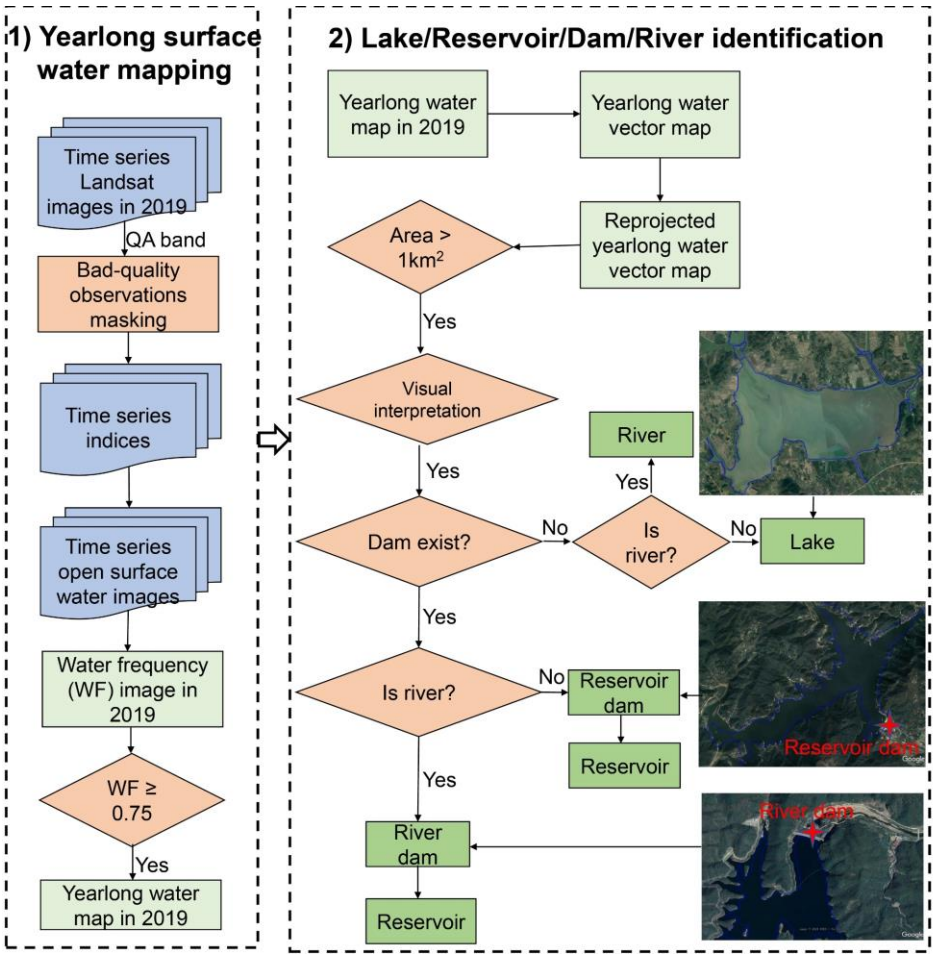
1) Yearlong surface water mapping
Time series Landsat images in 2019
QA band
Bad-quality observations masking
Time series indices
Time series open surface water images
Water frequency (WF) image in 2019
WF ≥ 0.75
Yes
Yearlong water map in 2019
2) Lake/Reservoir/Dam/River identification
Yearlong water map in 2019
Yearlong water vector map
Reprojected yearlong water vector map
Area > 1km²
Yes
Visual interpretation
Yes
River
Yes
Dam exist?
No
Is river?
No
Lake
Yes
Is river?
No
Reservoir dam
Reservoir
Reservoir dam
Yes
River dam
Reservoir
River dam

748

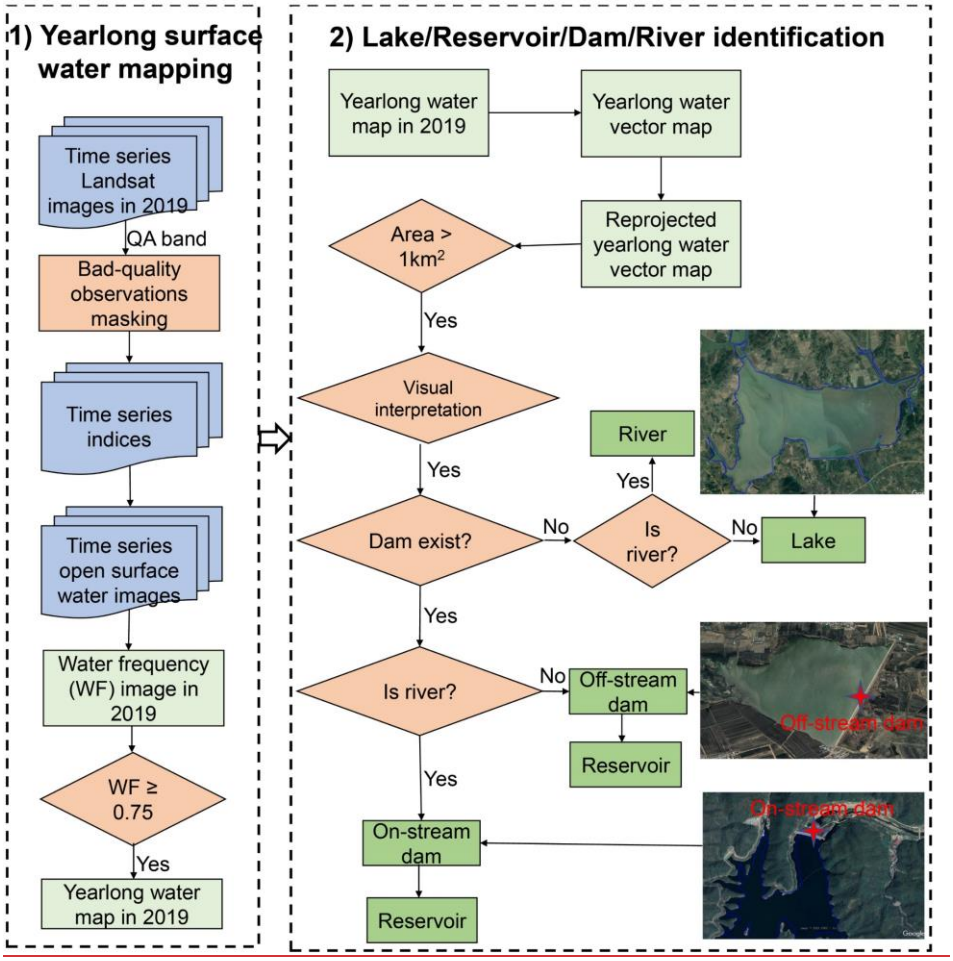

Fig. 43. Schematic flowchart of lakes, reservoirs, dams, and rivers identification in this study. The images were acquired from Google Earth Pro (© Google Earth Pro 2019).

设置了格式：字体：非加粗

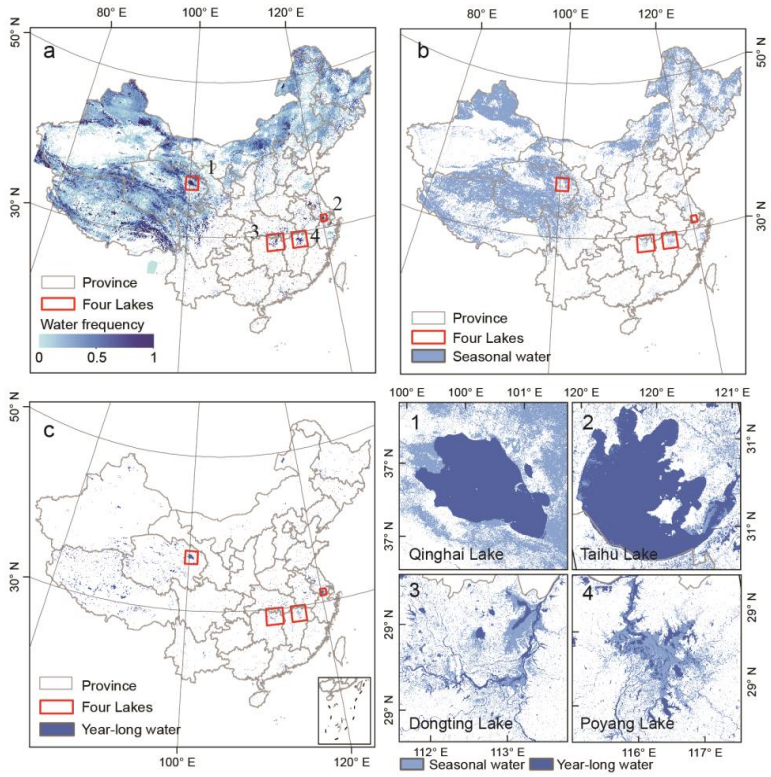
a
b
c
1
2
3
4
Province
Four Lakes
Water frequency
0
0.5
1
Seasonal water
Year-long water
Qinghai Lake
Taihu Lake
Dongting Lake
Poyang Lake
80° E
100° E
120° E
50° N
30° N
100° E
101° E
121° E
37° N
31° N
29° N
112° E
113° E
116° E
117° E

752

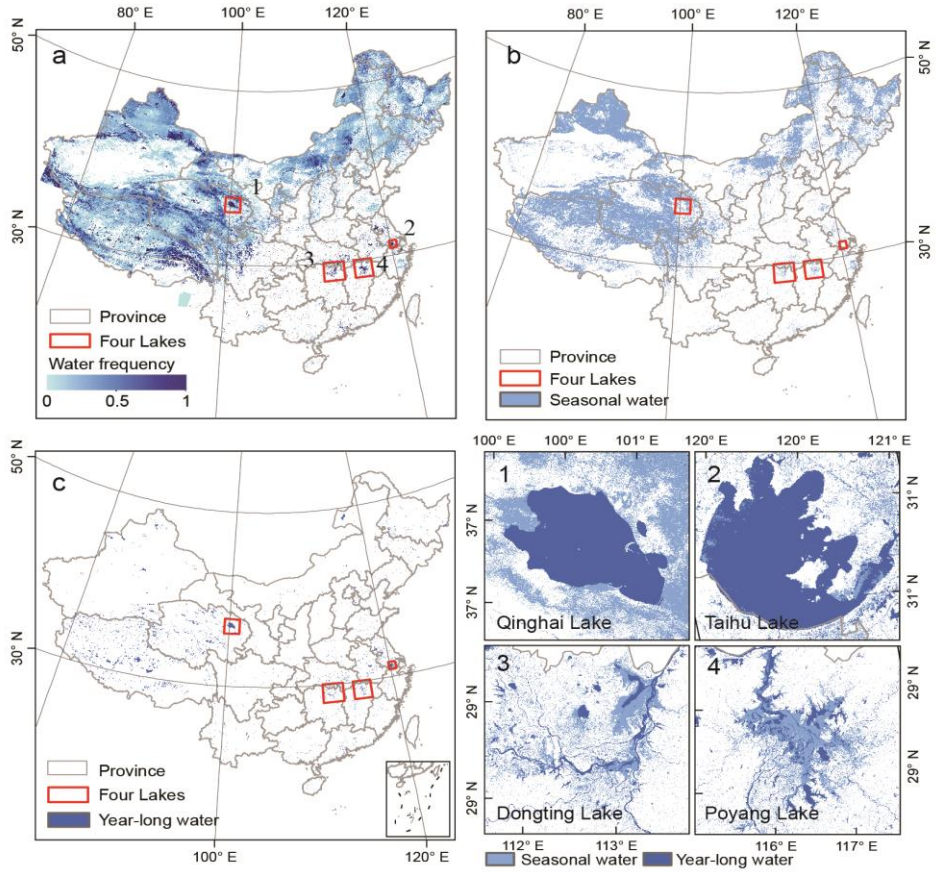

753

754 **Fig. ~~5~~4.** Spatial distribution of surface water body (SWB) in China for 2019. (a), Water frequency,

755 (b), Seasonal SWB, (c), Yearlong SWB. Subfigures (1-4) are three zoom-in views of seasonal and

756 year-long SWB in Qinghai Lake, Taihu Lake, Dongting Lake, and Poyang Lake in China.

设置了格式: 字体：非加粗

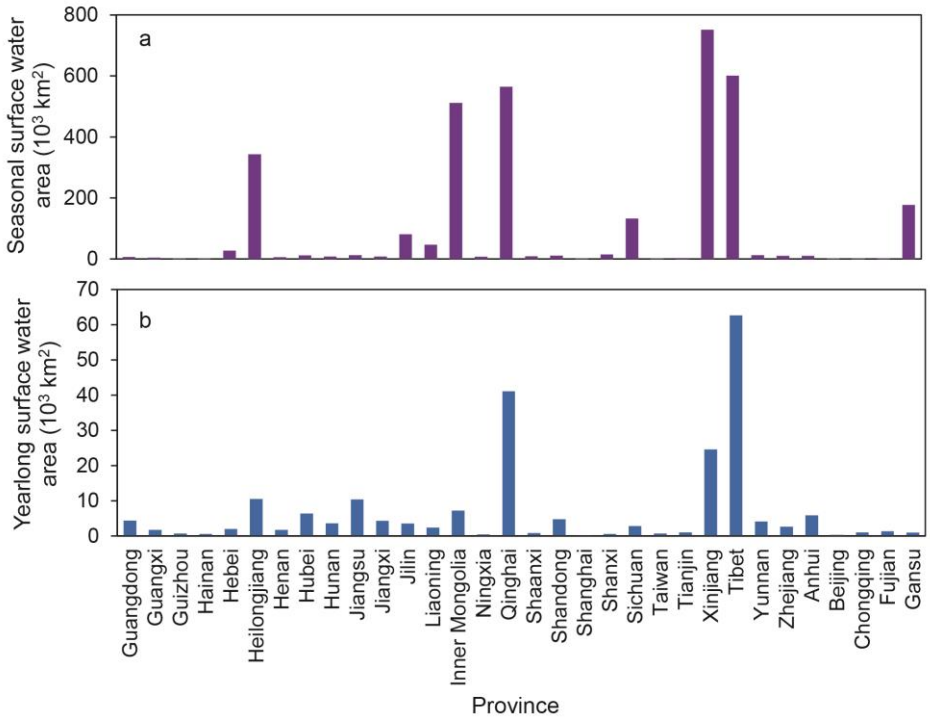
a
Seasonal surface water area (10^3 km^2)
800
600
400
200
0
b
Yearlong surface water area (10^3 km^2)
70
60
50
40
30
20
10
0
Guangdong
Guangxi
Guizhou
Hainan
Hebei
Heilongjiang
Henan
Hubei
Hunan
Jiangsu
Jiangxi
Jilin
Liaoning
Inner Mongolia
Ningxia
Qinghai
Shaanxi
Shandong
Shanghai
Shanxi
Sichuan
Taiwan
Tianjin
Xinjiang
Tibet
Yunnan
Zhejiang
Anhui
Beijing
Chongqing
Fujian
Gansu
Province

757

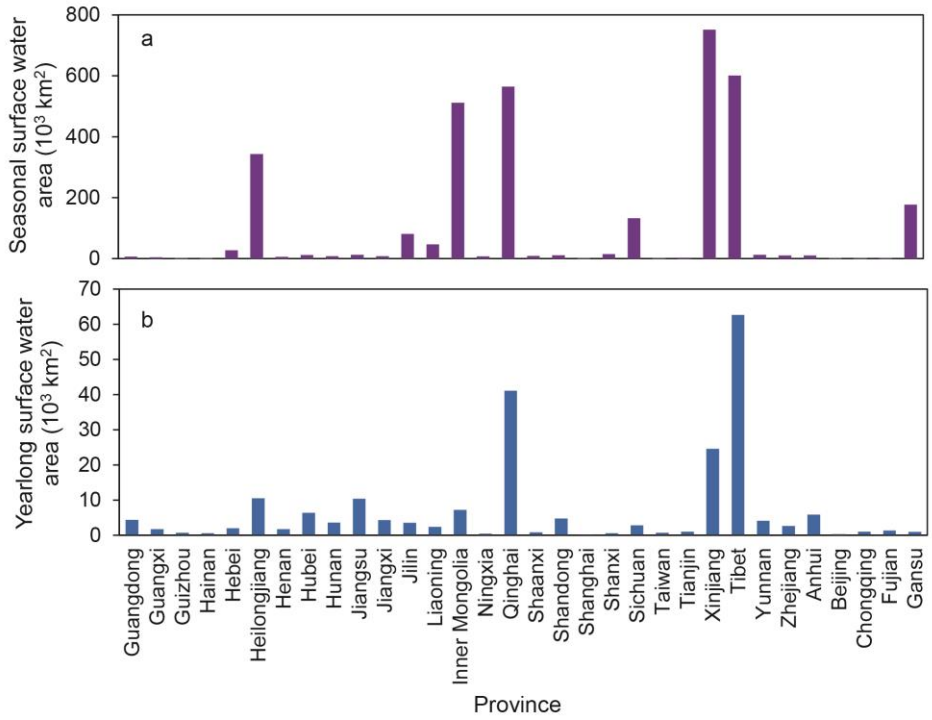

Fig. ~~6~~5. Areas of seasonal (a) and yearlong (b) surface water bodies by province in China for 2019.

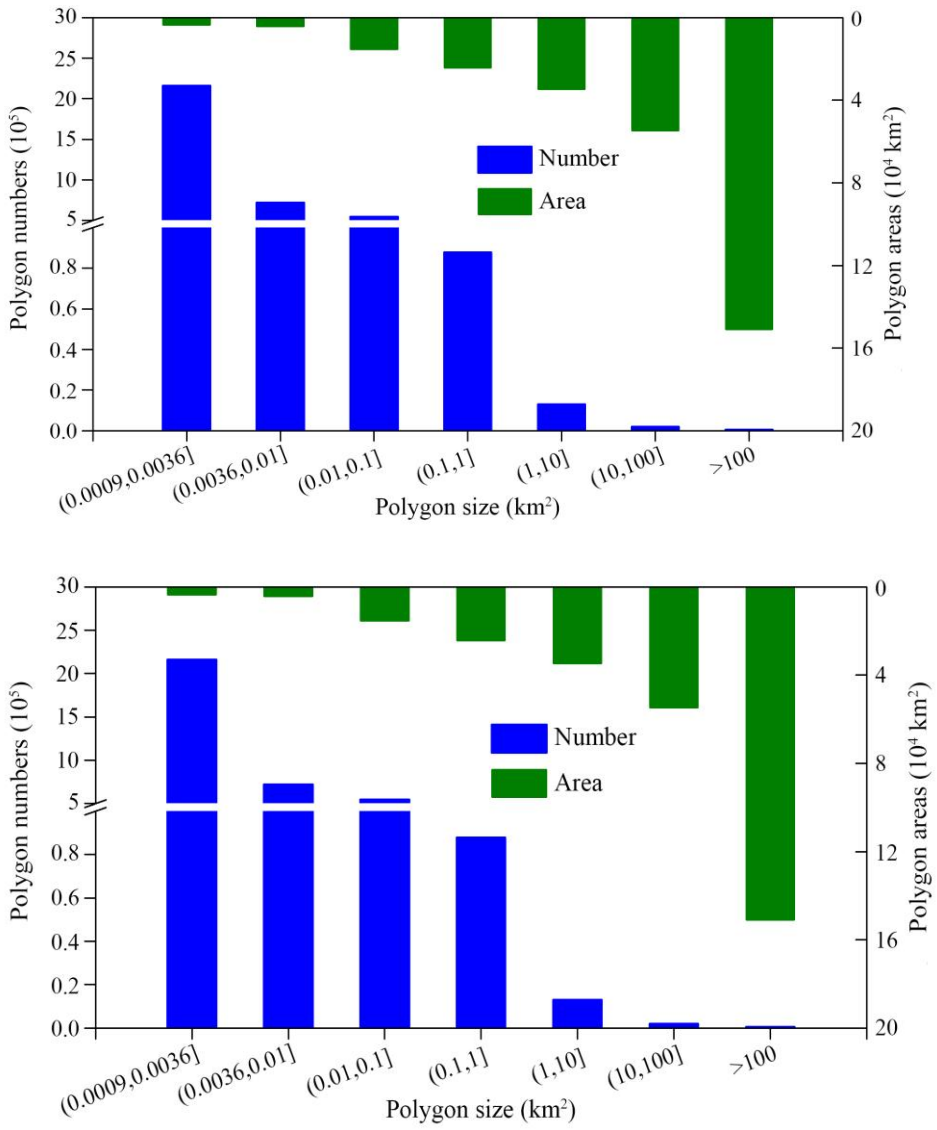

Fig. ~~7~~6. Numbers and areas of yearlong surface water body polygons with different sizes.

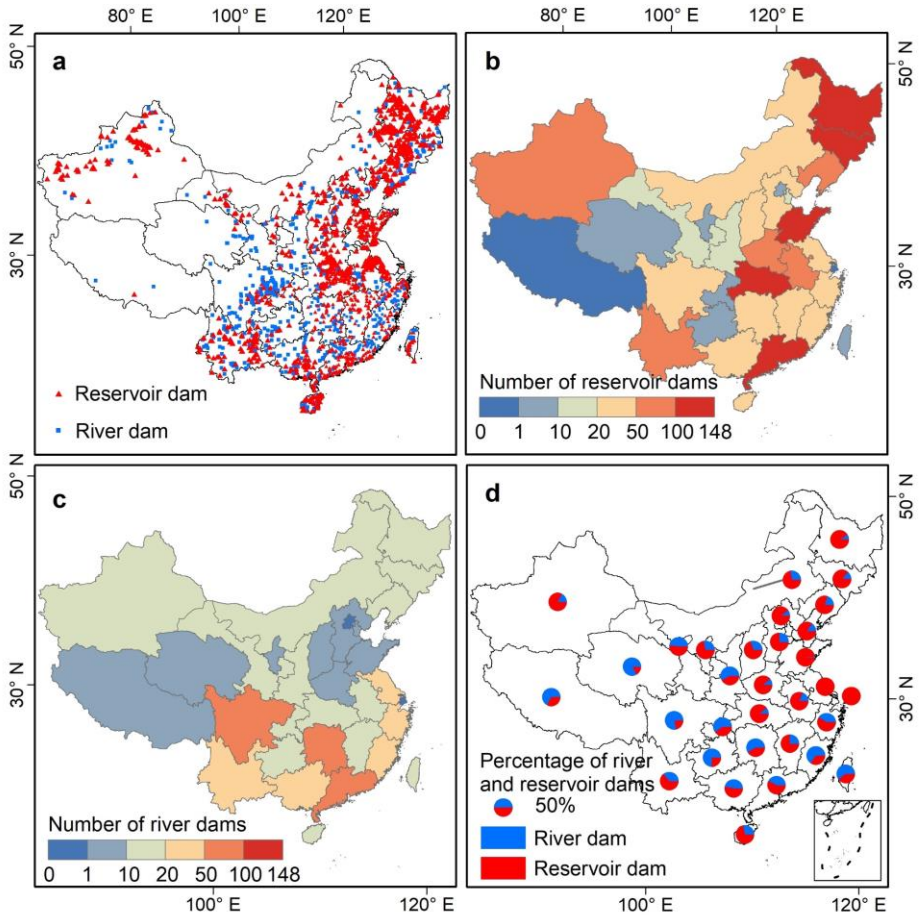
80° E
100° E
120° E
50° N
30° N
a
Reservoir dam
River dam
b
Number of reservoir dams
0 1 10 20 50 100 148
c
Number of river dams
0 1 10 20 50 100 148
d
Percentage of river and reservoir dams
50%
River dam
Reservoir dam

763

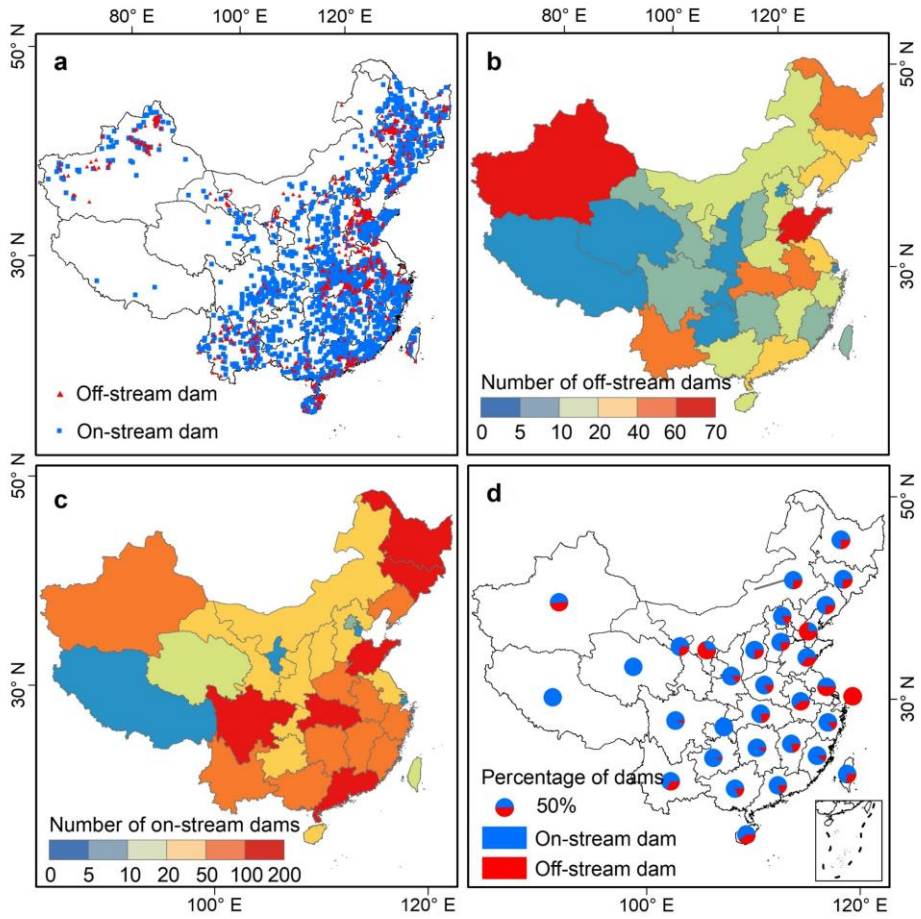

764

765 **Fig. ~~8~~7.** Distribution of ~~river dams~~off-stream and ~~reservoir~~on-stream dams in China for 2019. a,

766 Spatial distribution of ~~river dams and reservoir~~ dams; b, Number of ~~reservoir~~off-stream dams by

767 province; c, Number of ~~river~~on-stream dams by province; d, Percentage of ~~river dams~~off-stream

768 and ~~reservoir~~on-stream dams by province.

设置了格式：字体：非加粗

设置了格式：字体：非加粗

设置了格式：字体：非加粗

设置了格式：字体：非加粗

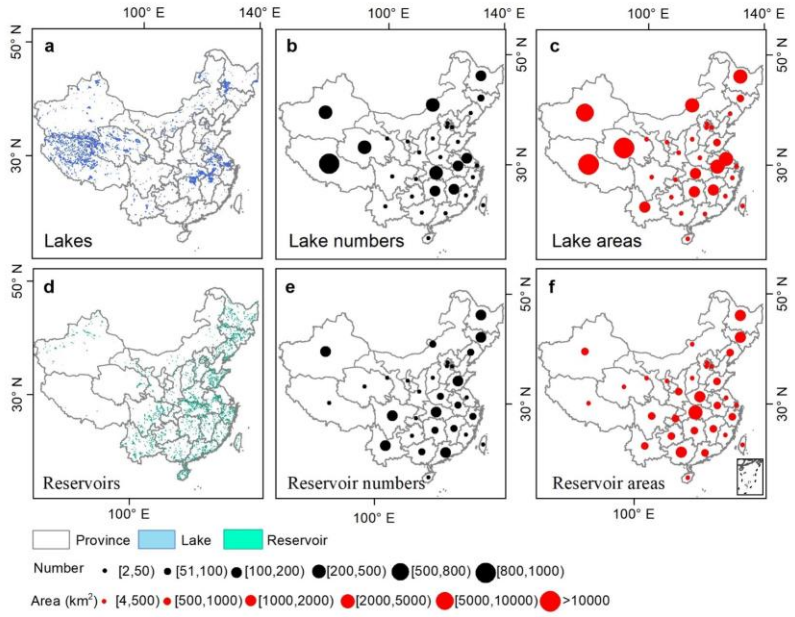
a
Lakes
b
Lake numbers
c
Lake areas
d
Reservoirs
e
Reservoir numbers
f
Reservoir areas
100° E
140° E
50° N
30° N
Province
Lake
Reservoir
Number
[2,50)
[51,100)
[100,200)
[200,500)
[500,800)
[800,1000)
Area (km²)
[4,500)
[500,1000)
[1000,2000)
[2000,5000)
[5000,10000)
>10000

769

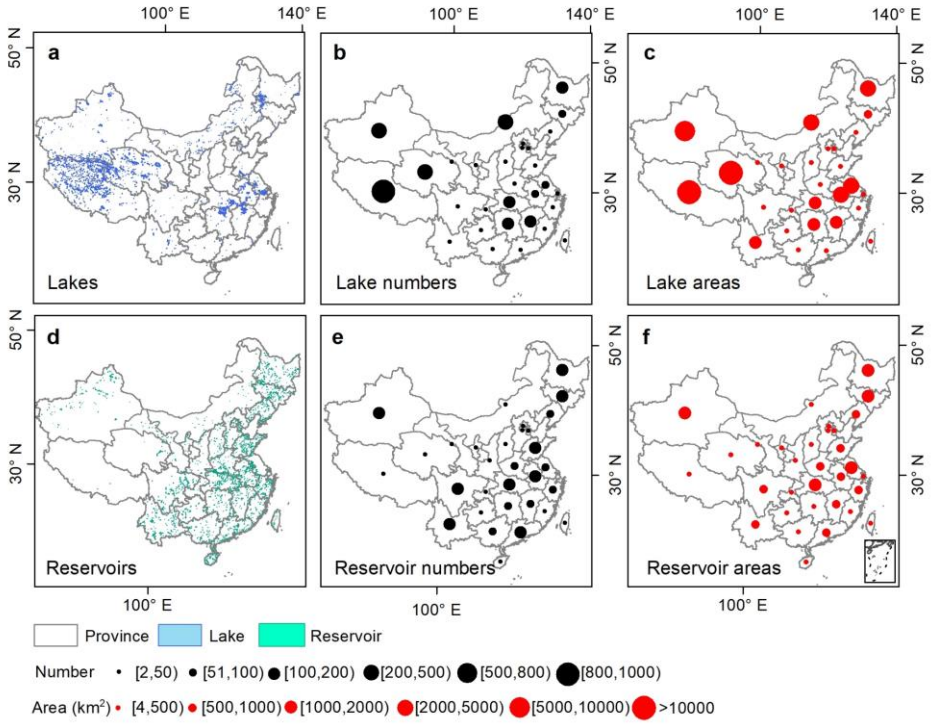

Fig. ~~9. Distribution~~8. Numbers and areas of lakes and reservoirs in China for 2019. a, Spatial distribution of lakes; b, Lake numbers by province; c, Lake areas by province; d, Spatial distribution of reservoirs; e, Reservoir numbers by province; f, Reservoir areas by province.

设置了格式：字体：非加粗

设置了格式：字体：非加粗

设置了格式：字体：非加粗

设置了格式：字体：非加粗

设置了格式：字体：非加粗

设置了格式：字体：非加粗

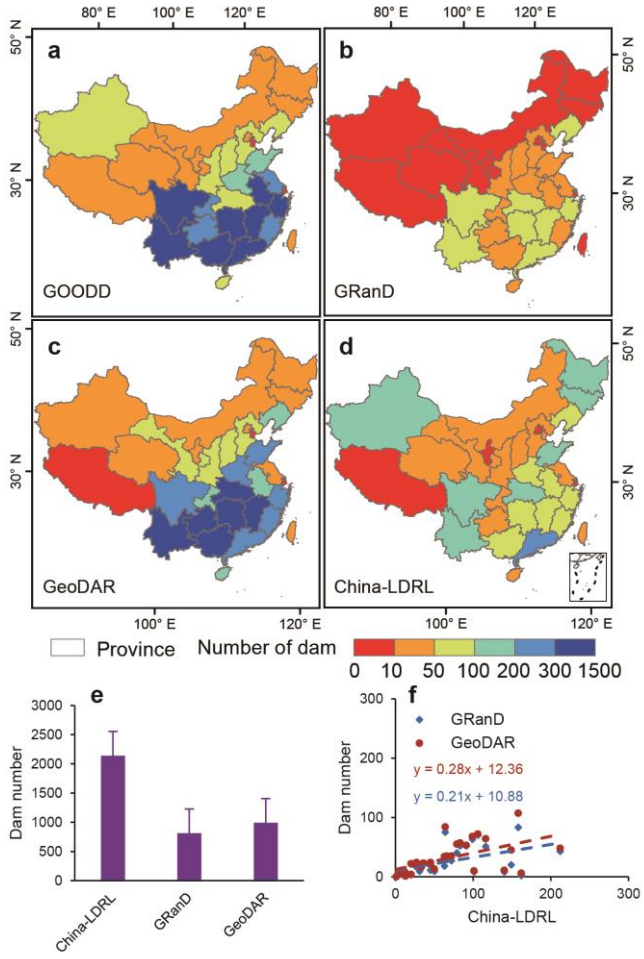
a
GOODD
b
GRanD
c
GeoDAR
d
China-LDRL
80° E
100° E
120° E
50° N
30° N
Province
Number of dam
0 10 50 100 200 300 1500
e
Dam number
3000
2500
2000
1500
1000
500
0
China-LDRL
GRanD
GeoDAR
f
GRanD
GeoDAR
y = 0.28x + 12.36
y = 0.21x + 10.88
Dam number
300
200
100
0
China-LDRL

774

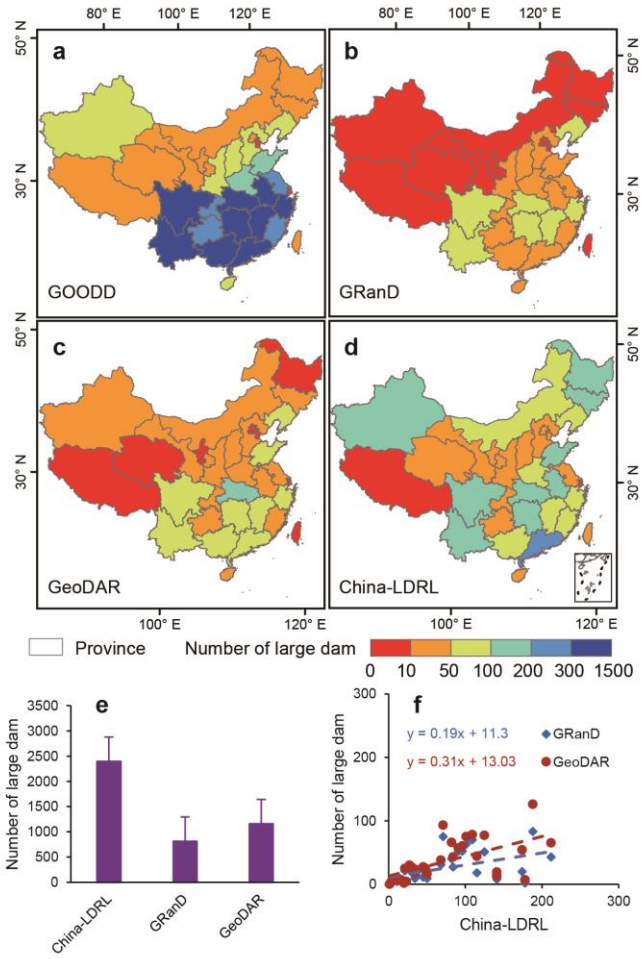

775

776 **Fig. ~~10~~9.** Numbers of large dams (with reservoir area > 1 km^2) of different datasets. (a) ~~Dam~~Large

777 dam number in the GOODD dataset ~~by province~~; (b) ~~Dam~~Large dam number in the GRanD dataset

778 ~~by province~~; (c) ~~Dam~~Large dam number in the GeoDAR dataset ~~by province~~; (d) ~~Dam~~Large dam

779 number in the China-LDRL dataset ~~by province~~; (e) ~~Large dam~~Total numbers of large dam from

780 different datasets in China; (f) The relationships of large dam numbers between China-LDRL ~~and~~,

设置了格式：字体：加粗

781 GRand and GeoDAR datasets.

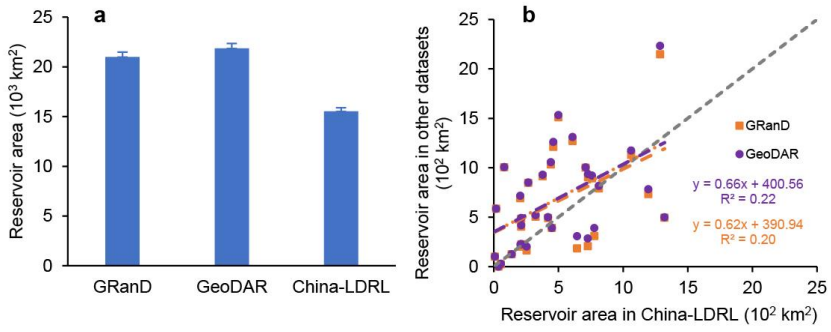

782

783

784 **Fig. ~~11.~~ ~~Areas of large reservoir (a) and their relationships (b) of the GRanD, GeoDAR, and our~~**

785 ~~China-LDRL datasets.~~

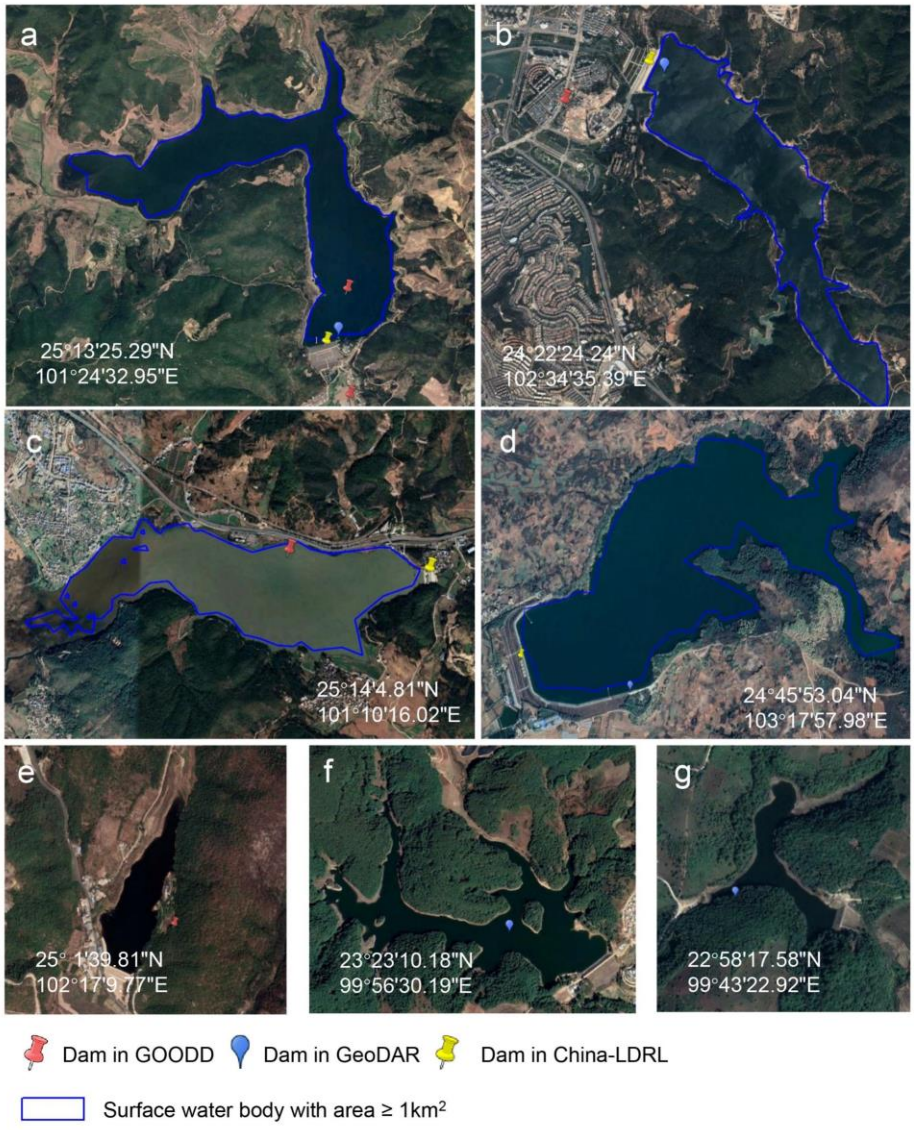

786

787 ~~Fig. 12. Dam~~**10.** Dams from the GOODD, GeoDAR, and China-LDRL datasets within Google

788 Earth Pro (© Google Earth Pro 2019).

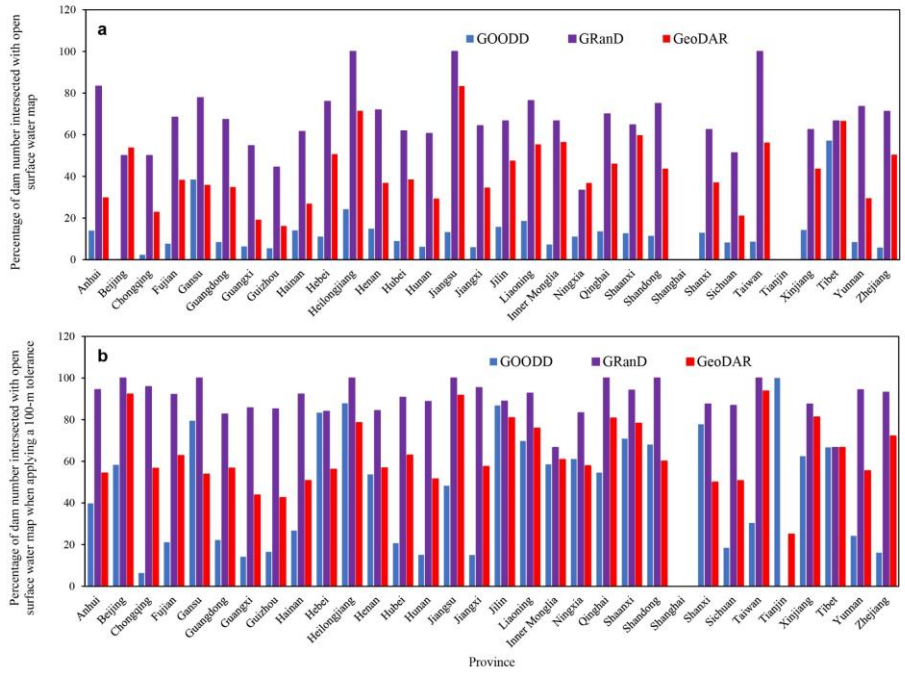

Fig. 13. The numbers of dams intersected with surface water body (SWB) map in China for 2019 by province. (a) Percentage of numbers of dams intersected with SWB map; (b) Percentage of numbers of dams intersected with SWB map when applying a 100-m tolerance.